Nuclear Matter and Dense Matter

Kuniharu Kubodera

University of South Carolina

WCU-Heavy Ion Meeting (HIM), May 28, 2010

Some pages in this set of slides were presented at the
WCU-APCTP Focus Workshop on May 26, 2010

Outline

1. Introduction — Nuclear matter observables
2. Phenomenological nucleon interactions
3. Effective Field Theory (EFT) appoach
4. Low-momentum NN potential — V_{lowk}
5. Brueckner-Goldstone approach to nuclear matter
6. Walecka model
7. Relativistic Brueckner-Hartree-Fock
8. Standard Nuclear Physics Approach (SNPA)

Introduction

Mass formula (Weizsäcker, 1935; Bethe and Bacher, 1936)
Binding energy of a nucleus ($A = Z + N$)

$$\mathcal{B}(N,Z) = b_{\rm vol} A - b_{\rm surf} A^{2/3} - \frac{1}{2} b_{\rm sym} \frac{(N-Z)^2}{A} - \frac{3}{5} \frac{Z^2 e^2}{R_c}$$

$$b_{\rm vol} \approx 16 \text{ MeV} \quad (1)$$

$$b_{\rm surf} \approx 17 \text{ MeV} \quad (2)$$

$$b_{\rm sym} \approx 50 \text{ MeV} \quad (3)$$

$$R_c \approx 1.24\, A^{1/3} \text{ fm} \quad (4)$$

For large A, the volume energy term dominates

$\equiv$ Saturation property

$\leftrightarrow$ Interactions are short-ranged

Range comparable to average inter-nucleon distance

Nuclear Matter, or (Symmetric) Nuclear Matter

Hypothetical system with $A \to \infty$,
$Z = N$ (symmetric matter)
Coulomb interaction turned off

Three "Observables" in Nuclear Matter

1. **Binding energy per nucleon**

$$\mathcal{B}/A = b_{\rm vol} = 16 \text{ MeV}$$

2. **Nuclear matter density –** ρ_0

Saturation property
$\to$ Almost uniform nucleon density in the core of heavy nuclei
$\to$ $\rho_0 \approx 0.16\,\text{nucleons/fm}^3$
$\to p_F = 0.27 \pm 0.01$ GeV/c
$\to k_F = 1.37\ \text{fm}^{-1}$

3. Compressibility of Nuclear Matter

$$K \equiv \left[k_F^2 \frac{d^2}{dk_F^2} \left(\frac{\mathcal{B}}{A} \right) \right]_{(k_F)_0} = 9 \left[\rho^2 \frac{\partial^2}{\partial \rho^2} \left(\frac{\mathcal{B}}{A} \right) \right]_{\rho_0}$$

The most frequently quoted "experimental value" of K:

$$K^{\rm exp} = 225 \pm 15 \text{ MeV}.$$

• **Extraction of $K^{\rm exp}$**

K is *not* a directly measurable quantity !

What one measures is the energy E_0 of the giant monopole resonance.

Define the **effective compression modulus** for a nucleus of mass number A via

$$E_0 = \sqrt{\frac{\hbar^2 A K_A}{m_N < r^2 >_0}}$$

Roughly speaking, we derive K using $K_A \overset{A \to \infty}{\longrightarrow} K$

Two methods — macroscopic and microscopic approaches

see e.g., Blaizot et al., NPA 591 (1995) 435

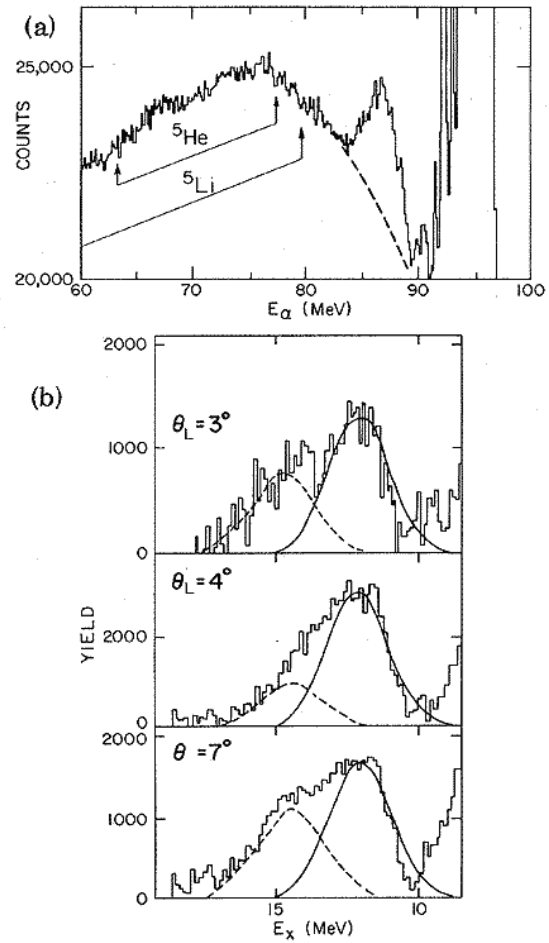

FIG. 1. (a) A ^{208}Pb(α,α') spectrum taken at $\theta_L = 4°$. The dashed line indicates the background chosen. (b) A portion of ^{144}Sm(α,α') spectra ($E_\alpha = 96$ MeV) taken at 3°, 4°, and 7° are shown after subtraction of the continuum background. Gaussian peaks are shown for both components utilizing positions and widths from Table I.

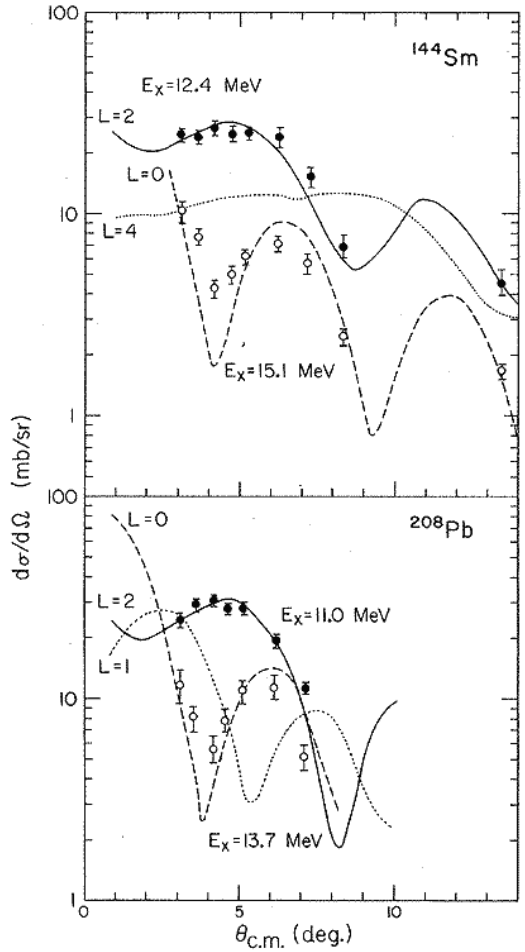

FIG. 2. Angular distributions obtained for both components of the giant resonance peaks in ^{144}Sm and ^{208}Pb. DWBA calculations are shown for several L transfers. The normalizations for the $L = 1$ and $L = 4$ calculations are arbitrary.

Youngblood, Rozsa, Moss, Brown, Bronson, Phys. Rev. Lett. 39, 1188-1191 (1977)

Macroscopic approach

- Motivated by the liquid drop model, we parameterize K_A as

$$K_A = K_{\rm vol} + K_{\rm surf} A^{-1/3} + K_{\rm sym} \left(\frac{N-Z}{A} \right)^2 + K_{\rm Coul} \frac{Z^2}{A^{4/3}}$$

- From data on E_0, deduce K_A and determine the coefficients in the above expression.
- This method does not lead to a very stringent determination of K:

$$K = 100 \sim 400 \ {\rm MeV}$$

In order to relate data on E_0 to K, one must know how the nucleus vibrates.

Microscopic approach

- Assume a phenomenological effective quasi-two-body interactions.
- Density-dependent delta-function — Skyrme forces
  [T.H.R. Skyrme, Nucl. Phys. 9 (1959) 615]
  $\longrightarrow$ Cogny effective interactions

$$
\begin{aligned}
V_{12} \quad = \quad & \sum_{i=1,2} (W_1 + B_i P_\sigma - H_i P_\tau - M_i P_\sigma P_\tau) \exp(-(r/\mu_i)^2) \\
& + t_3 (1 + x_3 P_\sigma) \rho^\alpha (\vec{R}) \delta(\vec{r}) + i W_0 (\sigma_1 + \sigma_2) \vec{k}' \times \delta(\vec{r}) \vec{k}
\end{aligned}
$$

- Density dependency
  $\longrightarrow$ reasonably successful description of finite nuclei *and* nuclear matter
- Carry out Hartree-Fock or Hartree-Fock-Bogoliubov calculations for various values of A, and nuclear matter
- Determine the parameters in the effective interactions using the observables, including E_0, for a range of mass numbers A
- Predict K.
  $\Rightarrow K^{\mathrm{exp}} = 225 \pm 15$ MeV.

- For a wide range of choices of the Cogny interactions, the above results are found to be reasonably stable.
- However, to what extent can we regard K as an experimentally measure quantity.
  As we will see, so much theoretical effort has been invested to explain the "empirical" value of "K" with the use of elaborate NN intertactions and many-body techniques.
- We can perhaps ask whether the existing method for deducing $K^{\rm exp}$ has matching accuracy.
- Some recent approaches use observables in heavy-ion collisions
  $\leftrightarrow$ I hope these will be discussed by experts of heavy-ion collisions at this Workshop

Phenomenological nucleon interactions

At long distances, attractive interactions due to pion exchange
At very short distances, strong repulsive interactions

- ^1S phase shift becomes negative at $E_{lab} \sim 250$ MeV
- ^3S phase shift becomes negative at $E_{lab} \sim 350$ MeV
- Strong repulsive force (over)compensating known attractive force

One way to represent this repusive force
$\rightarrow$ hard core (infinitely repulsive potential) of radius r_c

Construction of N-N potentials
Longest range part — one-pion exchange (well established)
Sub-long-range part — two-pion exchange
• Application of dispersion relations [Paris group (1973), Stony Brook group (1975)]

High-precision (phenomenological) N-N potentials

• Nijmegen NN scattering database

[Bergervoet et al. PRC 41 (1990); Stoks et al. PRC 48 (1993) 792]
1787 pp and 2514 np data in the Lab energy range 0-350 MeV

• A (modern) high-precision phenomenological NN potential fits this large basis of pp and np scattering data, and the deuteron properties, with $\chi^2/N \simeq 1$.

Nijmegen potential [Stoks et al., PRC (1994) 2950]

- One-pion exchange plus heavy boson exchanges with adjustable parameters
- These parameters are optimized individually for each of low partial waves.

CD-Bonn potential

[Machleidt, Holinde and Elster, Phys. Rep. 149 (1987) 1];
[Machleidt, Adv. Nucl. Phys. 19 (1989) 189];
[Machleidt, PRC 63 (2001) 024001]

- Contains one-pion exchange, ρ exchange, and ω exchange.
- Contains two scalar-isoscalar mesons (σ) in each partial wave up to $J = 5$.
- The mass and coupling constant of the second σ fine-tuned in each partial wave.
- Hadronic vertices regulated with form factors with cut-off ranging 1.3-1.7 GeV.
- With more restricted potential forms (OBEP-type), $\chi^2/N = 1.87$.

Argonne V18 (AV18) potential

[Wiringa, Stoks and Schiavilla, PRC 51 (1995) 38]

(Although isospin symmetry violation is a major concern in Wiringa et al., we suppress that feature here, for simplicity.) $\leftrightarrow$ Argonne v_{14} potential

- Assume a potential that is local in coordinate space.

$$v(r) = v^{\pi}(r) + v^{R}(r)$$

- $v^{\pi}(r)$ is the one-pion exchange potential with an exponential cutoff:

$$\begin{aligned} v^{\pi}(r) &= (\text{isospin factor}) \times [\, Y_{\mu}(r)\vec{\sigma}_1 \cdot \vec{\sigma}_2 + T_{\mu}(r) S_{ij} \,] \\ Y_{\mu}(r) &= \frac{e^{-m_{\pi} r}}{m_{\pi} r} \left(1 - e^{-cr^2}\right) \\ T_{\mu}(r) &= \left(1 + \frac{3}{m_{\pi} r} + \frac{3}{(m_{\pi} r)^2}\right) \frac{e^{-m_{\pi} r}}{m_{\pi} r} \left(1 - e^{-cr^2}\right)^2 \end{aligned}$$

- $v^{R}(r)$ is the remaining intermediate and short-range phenomenological part
- $v^{R}(r)$ is a sum of central, L^2, tensor, spin-orbit and quadratic spin-orbit terms in different S, T (and T_z) states

$$v^{R}_{ST} = v^{c}_{ST}(r) + v^{l2}_{ST}(r) L^2 + v^{t}_{ST}(r) S_{12} + v^{ls}_{ST}(r) \vec{L} \cdot \vec{S} + v^{ls2}_{ST}(r) (\vec{L} \cdot \vec{S})^2$$

Each radial function is given the general form:

$$
\begin{aligned}
v^i_{ST}(r) &= I^i_{ST} T^2_\mu(r) + [P^i_{ST} + m_\pi r Q^i_{ST} + (m_\pi r)^2 R^i_{ST}] W(r) \\
W(r) &= \left[1 + e^{(r-r_0)/a}\right]^{-1}
\end{aligned}
$$

- I^i_{ST}, P^i_{ST}, Q^i_{ST} and R^i_{ST} are parameters to be fit to data (with $c = 2.1$ fm^{-2}, $r_0 = 0.5$ fm, and $a = 0.2$ fm).
- There are 40 non-zero intermediate and short-range parameters
- $\chi^2/N_{\rm data} = 1.09$ for 4301 data in the range 0-350 MeV
- A prominent persisting problem — Deuteron quadrupole moment
  $(Q_d)_{\rm exp} = 0.2859(3)$ fm^2
  $(Q_d)_{\rm AV18} = 0.270$ fm^2
  $(Q_d)_{\rm AV18+Rel+MEC} = 0.275$ fm^2

Three-nucleon forces — V_{3N}

- Their existence is expected from the existence of irreducible Feynman diagrams involving three nucleons
- First explicit calculation – Fujita-Miyazawa V_{3N} (1957) — pion-nucleon scattering sandwiched between two nucleons
- **To what extent does V_{3N} affect nuclear observables ?**
- 3N interactions needed to describe the nuclear binding energies and levels
- It is now established that, in nonrelativisitc treatments of nuclear systems (see below), with realistic V_{2N} alone, the s-shell nuclei are underbound, whereas nuclear matter tends to be overbound at too high an equilibrium density.
- Recent (phenomenological) V_{3N}:
  Tucson-Melborne 3NF [McKeller and Rajaraman, 1968, Coon et al., 1975]
  Brazilian 3NF [Coelho et al., 1983]
  Urbana-Illinois 3NF [Pudliner et al., 1997, Pieper et al., 2001]

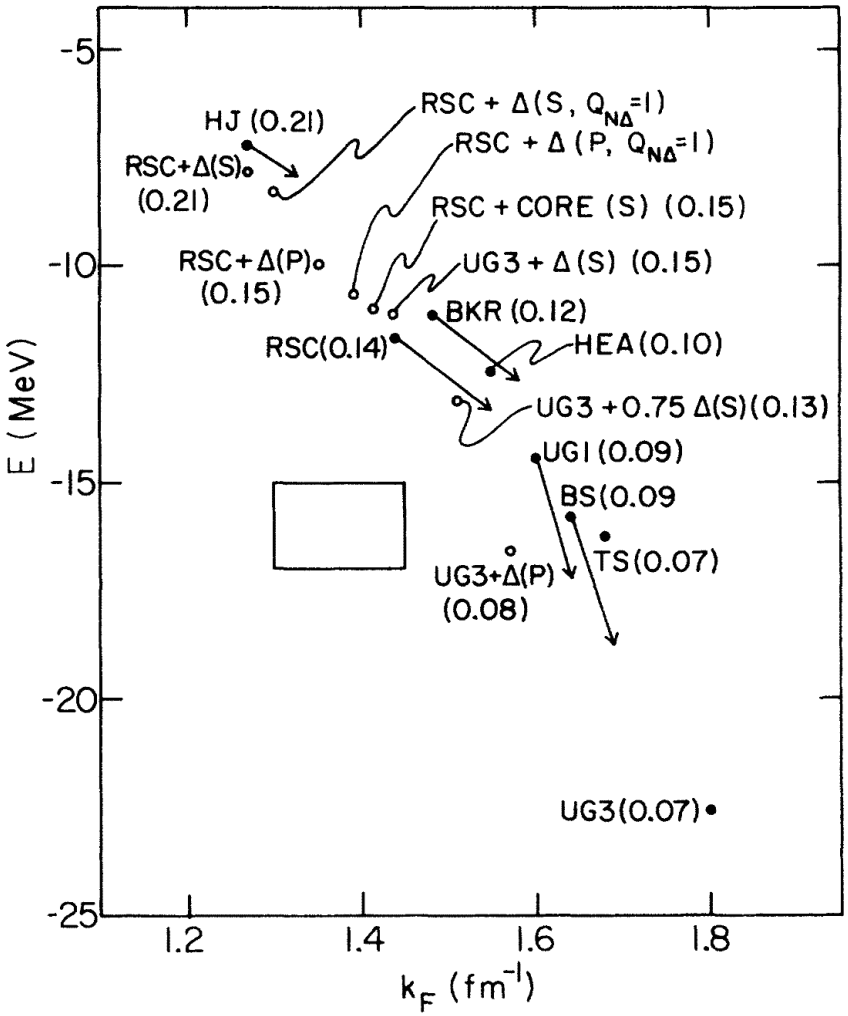

FIG. 1. Calculated saturation points for various models of the nucleon-nucleon interaction. The vertical axis is energy per particle in MeV, and the horizontal axis is Fermi momentum k_F in fm^{-1}. The value of the dimensionless defect parameter κ is given in parentheses. The quoted values of κ are evaluated at $k_F = 1.36$ fm^{-1}, *not* at the saturation densities, in order to permit meaningful comparison between different potentials.

Day and Coester, Phys. Rev. C 13, 1720 (1976)

- As an example, we explain the Urbana model,
  [Carlson, Pandharipande and Wiringa, NPA 401 (1983) 59]

$$V_{3N} = V_{3N2\pi} + V_{3NR}$$

  - $V_{3N2\pi}$: two-pion exchange contributions (motivated by Feynman diagrams)
  - V_{3NR} : purely phenomenological, **repulsive** 3NF introduced to improve the saturation property of nuclear matter

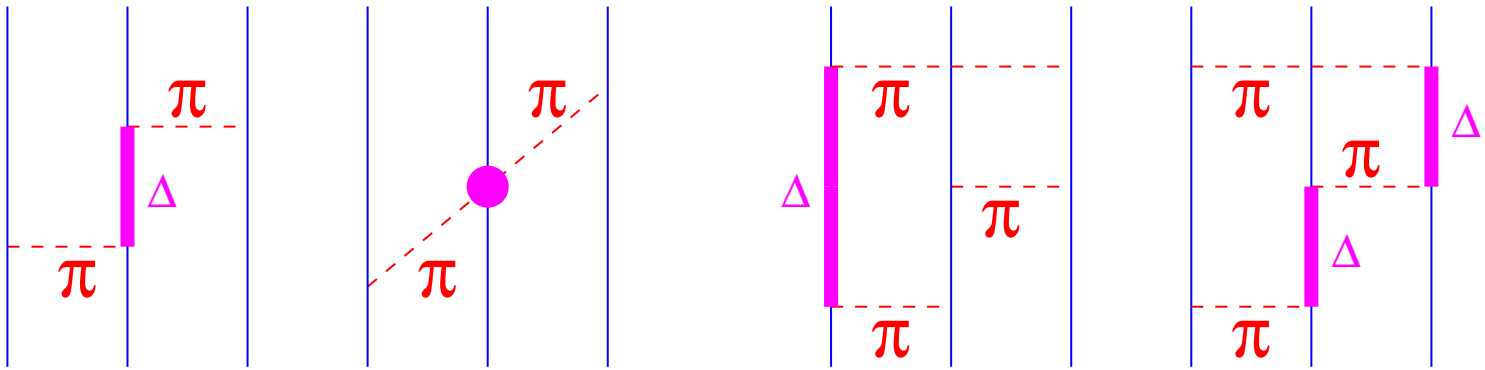

Figure: Terms in the Illinois three-nucleon potentials. S. C. Pieper Nucl.Phys. A751 (2005) 516

$$
\begin{aligned}
V_{3N2\pi} &= \sum_{\text{cycl.}} A_{2\pi}\{\vec{\tau}_1\cdot\vec{\tau}_2\,,\vec{\tau}_1\cdot\vec{\tau}_3\} \\
&\quad\times\{\,(S_{12}T(r_{12})+\vec{\sigma}_1\cdot\vec{\sigma}_2Y(r_{12})\,),(S_{13}T(r_{13})+\vec{\sigma}_1\cdot\vec{\sigma}_3Y(r_{13}))\} \\
&\quad+C_{2\pi}[\vec{\tau}_1\cdot\vec{\tau}_2\,,\vec{\tau}_1\cdot\vec{\tau}_3] \\
&\qquad\times[\,(S_{12}T(r_{12})+\vec{\sigma}_1\cdot\vec{\sigma}_2Y(r_{12})\,),(S_{13}T(r_{13})+\vec{\sigma}_1\cdot\vec{\sigma}_3Y(r_{13}))] \\
&\quad+B(\vec{r}_{12},\vec{r}_{13})\{\vec{\tau}_1\cdot\vec{\tau}_2\,,\vec{\tau}_1\cdot\vec{\tau}_3\}\{(S_{12}+\vec{\sigma}_1\cdot\vec{\sigma}_2),(S_{13}+\vec{\sigma}_1\cdot vsig_3))\} \\
Y(r) &= \frac{\mathrm{e}^{-\mu r}}{\mu r}Y_{\text{cut}}(r) \\
T(r) &= \left(1+\frac{3}{\mu r}+\frac{3}{\mu^2r^2}\right)\frac{\mathrm{e}^{-\mu r}}{\mu r}T_{\text{cut}}(r)
\end{aligned}
$$

$B(\vec{r}_{12},\vec{r}_{13})$ term comes from πN S-wave scattering.

- In the simple Δ intermediate-state model

$$\begin{aligned} A_{2\pi} &= -\left(\frac{f f^* m_\pi}{12\pi}\right)^2 \frac{2}{2E_{\rm av}} \sim -0.02\ {\rm MEV} \\ C_{2\pi} &= A_{2\pi}/4\,, \quad B(\vec{r}_{12},\vec{r}_{13}) = 0 \end{aligned}$$

  f $(f^*) = \pi NN$ $(\pi N\delta)$ coupling constant

- Tuscon group uses off-shell extrapolations of the πN scattering amplitude:

$$A_{2\pi} \sim -0.063\,{\rm MeV}\,, \quad C_{2\pi} \sim -0.018\,{\rm MeV}\,, \quad B(\vec{r}_{12},\vec{r}_{13}) \neq 0$$

Three main uncertainties in $V_{3N2\pi}$

(i) Its trength is not uniquely known.

(ii) V_{3N} gives major contributions via correlations induced by one-pion exchange potential between two nucleons But there are other (Goldstone) diagrams which are of similar nature and can give comparable contributions.

(iii) Short-range cutoffs in $Y(r)$ and $T(r)$ have ambiguity — They can reflect not only the πN form factors but also diagrams involving exchanges of heavier mesons.

Short-range repulsive part, V_{3NR}

- Generally the nuclear matter $E(k_f)$ does not saturate satisfactorily with Hamiltonian $v_{14} + V_{3N2\pi}$
- In-medium self-energy type diagrams can in principle generate repulsive effects
- This contribution is estimated to be of the order of $(U_\Delta - U_N)P_\Delta$, where U_Δ (U_N) is the real optical potential of a Δ (nucleon) in nuclear matter ($P_\Delta =$ isobar percentage in nuclear matter.)
- The suggested form of V_{3NR} of intermediate range is

$$V^I_{3NR} = U_0 \sum_{\text{cycl.}} T^2(r_{12})T^2(r_{13})$$

- This type of "derivation" of V_{3NR} is very inconclusive.
- As a *purely phenomenological* alternative, one may consider a short-range V_{3NR} given by

$$\begin{aligned} V^S_{3NR} &= U_C W(r_{12})W(r_{13})W(r_{23})\,, \\ W(r) &= [1+\exp\{(r-R)/c\}]^{-1}\,, \quad R = 0.5\,\text{fm}\,, \quad c = 0.2\,\text{fm} \end{aligned}$$

The "Woods-Saxon" form, $W(r)$, describes the core of the v_{14} NN potential.

High-precision phenomenological N-N potentials
— highly successful in many ways

However:

- It is difficult to assign reliable estimates of theoretical uncertainties.
- Gauge and chiral symmetry are difficult to implement.
- Three-nucleon forces cannot be introduced systematically.
- Connection to QCD is not obvious.
  $\Longleftrightarrow$ Effective field theory approach to nuclear forces

Effective field theory (EFT)

- Low energy-momentum phenomena characterized by a scale Q:
  Cut-off scale $\Lambda_{\rm cut} \gg Q$
- Retain only low energy-momentum degrees of freedom (effective fields $\phi_{\rm eff}$).
  $\Rightarrow$ Effective Lagrangian $\mathcal{L}_{\rm eff}$, which consists of monomials of $\phi_{\rm eff}$ and its derivatives consistent with the symmetries.
- A term involving n derivatives $\sim (Q/\Lambda_{\rm cut})^n$
  $\Rightarrow$ perturbative series in $Q/\Lambda_{\rm cut}$.
- The coefficient of each term – low-energy constant (LEC):
  LECs subsume high energy dynamics
  If the LEC's up to a specified order n are known
  $\leftrightarrow$ $\mathcal{L}_{\rm eff}$ serves as a complete (and hence model-independent) Lagrangian.
- The results obtained have accuracy of order $(Q/\Lambda_{\rm cut})^{n+1}$.
- In our case, $\mathcal{L}_{\rm QCD} \to \mathcal{L}_{\chi\rm PT}$ [Chiral Perturbation Theory (χPT)]
  In $\mathcal{L}_{\chi\rm PT}$, nucleons and pions are the effective degrees of freedom — $\Lambda_{\rm cut} \sim 1$ GeV.

- A system involving a nucleon $\leftrightarrow$ heavy-baryon chiral perturbation theory (HBχPT) [Jenkins and Manohar (1991)]
- HBχPT cannot be applied in a straightforward manner to nuclei.
  $\Leftrightarrow$ The existence of very low-lying excited states in nuclei
- *Nuclear* χPT à la Weinberg (1990)
  - Classify Feynman diagrams into two groups.
    Irreducible diagram – Every intermediate state has at least one meson in flight
    Reducible diagrams – Diagrams that are nor irreducible
  - Apply the chiral counting rules only to irreducible diagrams.
  - Treat irreducible diagrams (up to a specified chiral order) as an effective potential (to be denoted by $V_{ij}^{\rm EFT}$) acting on nuclear wave functions.
  - Incorporate reducible diagrams by solving the Schrödinger equation

$$H^{\rm EFT}|\Psi^{\rm EFT}> = E|\Psi^{\rm EFT}>,$$

$$H^{\rm EFT} = \sum_{i}^{A} t_i + \sum_{i<j}^{A} V_{ij}^{\rm EFT} + \sum_{i<j<k}^{A} V_{ijk}^{\rm EFT}$$

NN force at lowest chiral order

$$
\begin{aligned}
\mathcal{L}_{\pi}^{(0)} &= \frac{F^2}{4}[\nabla^{\mu}U\nabla_{\mu}U^{\dagger}+\chi_{+}] \\
\mathcal{L}_{\pi N}^{(0)} &= \bar{N}[\,iv\cdot D+\mathring{g}_A\,u\cdot S]N \\
\mathcal{L}_{NN}^{(0)} &= -\frac{1}{2}C_S(\bar{N}N)(\bar{N}N)+2\,C_T(\bar{N}SN)(\bar{N}SN)
\end{aligned}
$$

F = pion decay constant
$U(\vec{\pi})=u^2(\vec{\pi})=\exp\,(i\frac{\vec{\tau}\cdot\vec{\pi}}{F})=1+i\frac{\vec{\tau}\cdot\vec{\pi}}{F}-\frac{1}{2F^2}\vec{\pi}^2+\mathcal{O}(\vec{\pi}^3)$
v_μ = nucleon four-vector (usually v_μ =(1,0,0,0))
$S_\mu\equiv(1/2)i\gamma_5\sigma_{\mu\nu}v^\nu,\;\; D_\mu=\partial_\mu+[u^\dagger,\partial_\mu u]/2,\;\; u_\mu=i(u^\dagger\partial_\mu-u\partial_\mu u^\dagger)$
$\chi_+=u^\dagger\chi u^\dagger+u\chi^\dagger u,$
with $\chi=2B\mathcal{M}$ and $\mathcal{M}=\mathrm{diag}(m_u,m_d)$, $<0|\bar{u}u|0>=-F^2B$

- Expand $\mathcal{L}_{\pi}^{(0)}$ in powers of the pion fields, and organize diagrams according to their chiral powers

- Leading order (LO) contibutions ($\nu = 0$)
  There are only two possible connected two-nucleon tree diagrams:
  One-pion exchange diagram + Contact diagram

$$V_{2N}^{(0)} = -\frac{g_A^2}{4F_\pi^2}\frac{\vec{\sigma}_1 \cdot \vec{q}\,\vec{\sigma}_2 \cdot \vec{q}}{\vec{q}^2 + M_\pi^2}\vec{\tau}_1 \cdot \vec{\tau}_2 + C_S + C_T\vec{\sigma}_1 \cdot \vec{\sigma}_2$$

$\vec{q} = \vec{p}' - \vec{p}$, $F_\pi = 92.4$ MeV (pion decay constant), g_A=1.267.

- It turns out that there are no $\nu = 1$ contributions.

Leading order

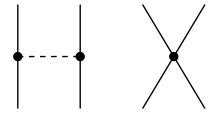

Next–to–leading order

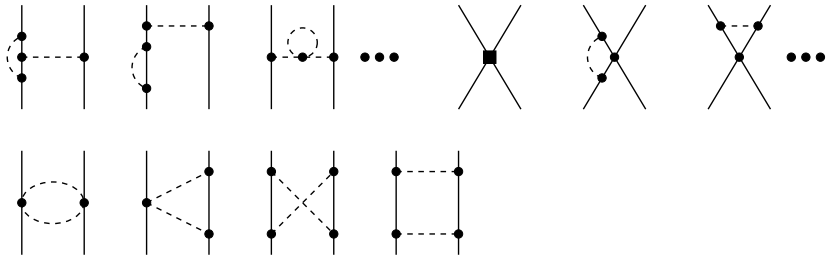

Next–to–next–to–leading order

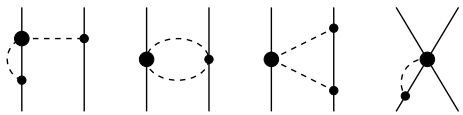

Next–to–next–to–next–to–leading order

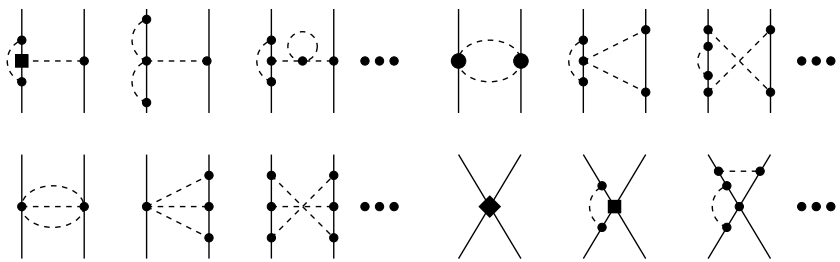

Figure: Chiral expansion of the two-nucleon force up to N^{3}LO. Solid dots, filled circles, squares and diamonds denote vertices with $\Delta_i = 0,\ 1,\ 2$ and 4, respectively. Only irreducible contributions of the diagrams are taken in to account.

Epelbaum, Hammer, Meißner, Rev.Mod.Phys.81:1773-1825, 2009

- $\nu = 2$ contributions (NLO)

$$
\begin{aligned}
\mathcal{L}_{\pi}^{(2)} &= \frac{l_3}{16} <\chi_+>^2 + \frac{l_4}{16}\Big(2 <\nabla_\mu U \nabla^\mu U^\dagger> \\
&\quad + 2 <\chi^\dagger U \chi^\dagger U + \chi U^\dagger \chi U^\dagger> -4 <\chi^\dagger \chi> - <\chi_->^2\Big) \\
\mathcal{L}_{\pi N}^{(2)} &= \bar{N}\left(\frac{1}{2\,\overset{\circ}{m}}(v\cdot D)^2 - \frac{1}{2\,\overset{\circ}{m}} D\cdot D + d_{16} S\cdot u <\chi_+> + i d_{18} S^\mu [D_\mu, \chi_-]\right) N \\
\mathcal{L}_{NN}^{(2)} &= \tilde{C}_1 [\,(\bar{N} D N)\cdot(\bar{N} D N) + ((D\bar{N})N)\cdot((D\bar{N})N)] \\
&\quad -2\,(\tilde{C}_1 + \tilde{C}_2)\,(\bar{N} D N)\cdot((D\bar{N})N) \\
&\quad -\tilde{C}_2\,(\bar{N} N)\cdot((D^2\bar{N})N) + \bar{N} D^2 N) + \ldots
\end{aligned}
$$

l_i, d_i and $\tilde{C}_i$ — additional LEC's

$\overset{\circ}{m}$ — nucleon mass in the chiral limit

Tree diagrams involving one $\nu = 2$ vertex, and loop diagrams involving only $\nu = 0$ vertices give rise to an NLO potential.

$$V_{2N}^{(2)} = -\frac{\vec{\tau}_1 \cdot \vec{\tau}_2}{384\pi^2 F_\pi^4} L^{\tilde{\Lambda}}(q) \left(4M_\pi^2(5g_A^4 - 4g_A^2 - 1) + \vec{q}^2(23g_A^4 - 10g_A^2 - 1) + \frac{48 g_A^4 M_\pi^4}{4M_\pi^2 + \vec{q}^2} \right)$$

$$- \frac{3\, g_A^4}{64\pi^2 F_\pi^4} L^{\tilde{\Lambda}}(q) (\vec{\sigma}_1 \cdot \vec{q}\, \vec{\sigma}_2 \cdot \vec{q} - \vec{\sigma}_1 \cdot \vec{\sigma}_2\, \vec{q}^2)$$

$$+ C_1 \vec{q}^2 + C_2 \vec{k}^2 + (C_3 \vec{q}^2 + C_4 \vec{k}^2) \vec{\sigma}_1 \cdot \vec{\sigma}_2 + i C_5 \frac{1}{2} (\vec{\sigma}_1 + \vec{\sigma}_2) \cdot \vec{q} \times \vec{k}$$

$$+ C_6\, \vec{q} \cdot \vec{\sigma}_1 \vec{q} \cdot \vec{\sigma}_2 \; + \; C_7 \vec{k} \cdot \vec{\sigma}_1 \vec{k} \cdot \vec{\sigma}_2$$

- $\nu = 3$ contributions (N^{2}LO) —
  The only contribution comes from the 2π-exchange triangle diagram

$$V_{2N}^{(3)} = -\frac{3\, g_A^2}{16\pi F_\pi^4} \left[2M_\pi^2(2c_1 - c_3) - c_3 \vec{q}^2 \right] (2M_\pi^2 + \vec{q}^2)\, A^{\tilde{\Lambda}}(q)$$

$$- \frac{g_A^2 c_4}{32\pi F_\pi^4} \vec{\tau}_1 \cdot \vec{\tau}_2 (4M_\pi^2 + q^2)\, A^{\tilde{\Lambda}}(q)\, (\vec{\sigma}_1 \cdot \vec{q}\, \vec{\sigma}_2 \cdot \vec{q} - \vec{\sigma}_1 \cdot \vec{\sigma}_2\, \vec{q}^2)$$

$A^{\tilde{\Lambda}}(q)$ — loop function

Short-range contributions due to c_3 very strong — A few tens of MeV at $r \sim M_\pi^{-1}$

$\leftrightarrow$ Δ-excitation diagram

The first non-vanishing contributions to 3NF occur at N^{2}LO

$$V_{3N}^{(3)} = \frac{g_A^2}{8F_\pi^4}\frac{\vec{\sigma}_1\cdot\vec{q}_1\vec{\sigma}_3\cdot\vec{q}_3}{(q_1^2+M_\pi^2)(q_3^2+M_\pi^2)}\Big[\vec{\tau}_1\cdot\vec{\tau}_3(-4c_1M_\pi^2+2c_3\vec{q}_1\cdot\vec{q}_3) + c_4\vec{\tau}_1\times\vec{\tau}_3\cdot\vec{\tau}_2\,\vec{q}_1\times\vec{q}_3\cdot\vec{\sigma}_2\Big] - \frac{g_AD}{8F_\pi^2}\frac{\vec{\sigma}_3\cdot\vec{q}_3}{q_3^2+M_\pi^2}\vec{\tau}_1\cdot\vec{\tau}_3\;\vec{\sigma}_1\cdot\vec{q}_3 + \frac{1}{2}E\,\vec{\tau}_2\cdot\vec{\tau}_3 + (\text{permutations})$$

$\vec{q}_i = \vec{p}_i\,' - \vec{p}_i$; $\vec{p}_i$ ($\vec{p}_i\,'$) = initial (final) momentum of the i-th nucleon;
The LEC, E, appears in

$$\mathcal{L}_{NNN}^{(1)} = -(1/2)(\bar{N}N)(\bar{N}\vec{\tau}N)\cdot(\bar{N}\vec{\tau}N)$$

- $\nu = 4$ contributions (N^{3}LO)

$$V_{4N}^{(4)} = \ldots\ldots$$

See Epelbaum, Hammer and Meissner, Rev. Mod. Phys. 81 (2009) 1773.

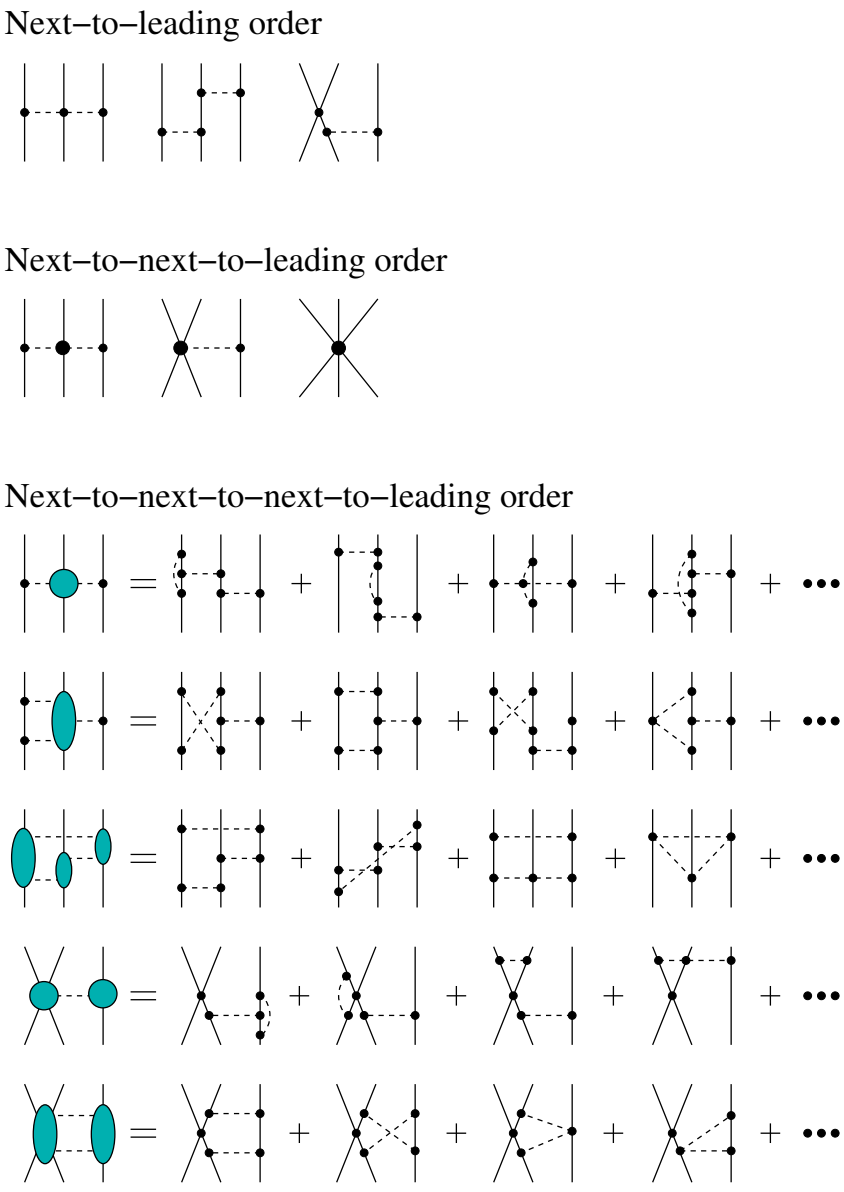

Figure: Chiral expansion of the three-nucleon force up to N^{3}LO. Diagrams in the first line (NLO) yield vanishing contributions to the 3NF if one uses energy-independent formulations as explained in the text. The five topologies at N^{3}LO involve the two-pion exchange, one-pion-two-pion-exchange, ring, contact-one-pion exchange and contact-two-pion-exchange diagrams in order. Shaded blobs represent the corresponding amplitudes.

Epelbaum, Hammer, Meißner, Rev.Mod.Phys.81:1773-1825, 2009

Relation between the well-established HBχPT nuclear interactions and scattering amplitudes — still actively debated !!

- Need to solve the Shrödinger or Lippmann-Schwinger (LS) equation within the cutoff
- The standard procedure (Wilsonian method) involves two steps:
  - **(1)** Solve the LS equation regularized with a finite cutoff in momentum (or coordinate) space, using as the kernel the potential truncated at a given chiral order
  - **(2)** Determine the LECs accompanying the contact terms in the potential by matching the resulting phase shifts to experimental data — This procedure can be regarded (in this framework) as renormalization.

The most advanced analyses of NN scattering based on the Weinberg power counting take into account the 2NF contributions up to N^{3}LO
— Entem and Machleidt, PRC 68 (2003) 041001
— Epelbaum, Glöckle and Meissner, NPA 747 (2005) 362

- Most of the LECs (c_is, d_is) entering into the long-range part (pion exchanges) well determined from the pion-nucleon system.

- 24 unknown LECs for the short-range part
  $\leftrightarrow$ determined from the low-energy NN data
  (for several choices of the cutoff for the Schrödinger equation)

  $\longrightarrow$ Accurate shase shifts for np scattering up to $E_{lab} \sim 200$ MeV.

- Up to ~ 200 MeV, remarkable stability against changes in the cutoff,
  $$\Lambda = 450 \ldots 600 \text{ MeV}$$

- For the channels that have the tensor force, the approach works only up to around 150 MeV.

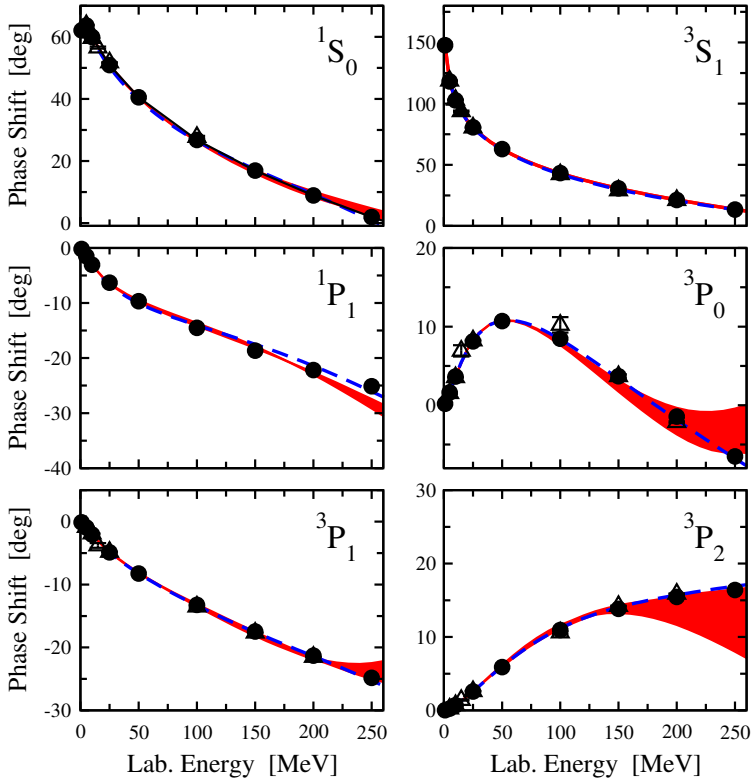

Figure: Neutron-proton phase shifts in S- and P-waves at N^{3}LO in comparison with the Nijmegen (filled circles) and Virginia Tech (open triangles) PWA.

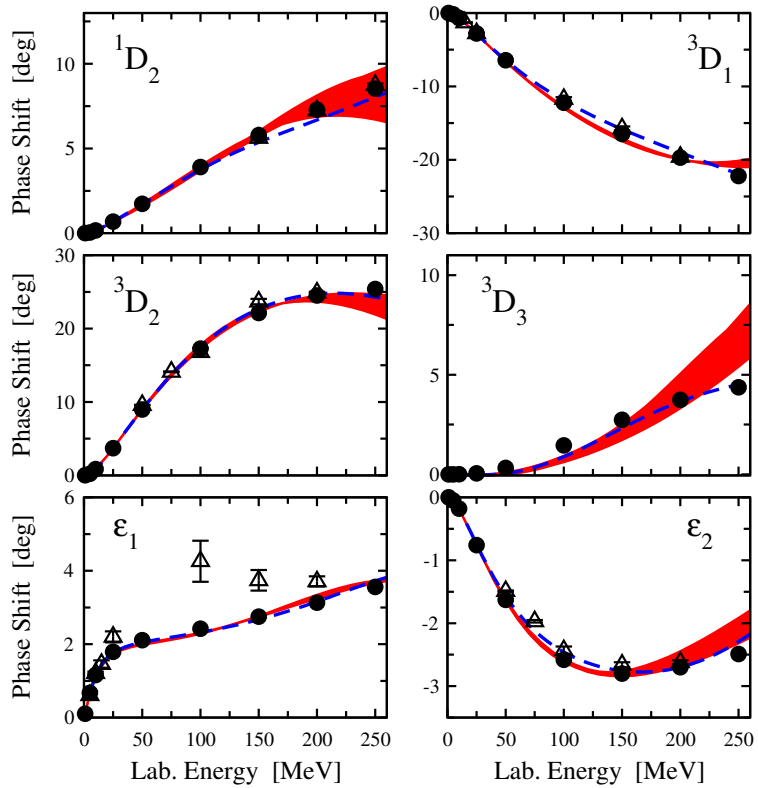

Figure: Neutron-proton phase shifts in D-waves and the mixing angles $\epsilon_{1,2}$ at N^{3}LO.

Epelbaum, Hammer, Meißner, Rev.Mod.Phys.81:1773-1825, 2009

Low-momentum N-N potential

Low-momentum N-N potential – $V_{\mathrm{low-k}}$

Bogner, Kuo and Schwenk, Phys. Rep. 386 (2003) 1

- Suppose we are interested in nuclear phenomena characterized by a momentum scale k, which is lower than a certain cut-off Λ.
- Low-momentum part (long-range part) fairly well described in terms of meson exchanges
  $\longrightarrow$ For this part, we may hope to achieve some degree of model independence.

Unitary-Model-Operator Approach (UMOA)

S. Okubo, Prog. Theor. Phys. 12 (1954) 603

- $P \equiv$ projector onto the model space of NN states with $k < \Lambda$, and $Q \equiv 1 - P$.
  Construct a unitary transformation U such that $Q(U^{-1}HU)P = 0$.
- Define $V_{\mathrm{eff}} = V_{lowk} \equiv U^{-1}(h_0 + V)U - h_0 \quad (h_0 = \text{kinetic energy})$
- Solving the Lippmann-Schwinger equation with V_{lowk} in P-space gives the same phase shifts as the oroginal L-S equation without cutoff.
  $\leftrightarrow$ V_{lowk} is as *realistic* a potential as the CD Bonn and Av18.

Renormalization Group (RG) Method

Kuo-Lee-Ratocliff (KLR) folded diagram series:

- Define an *energy-dependent* effective potential (called the $\hat{Q}$ box) that is irreducible with respect to cutting intermediate low-momentum propagators.
- The $\hat{Q}$ box contains the effects of the high momentum modes. The $\hat{Q}$ box is similar to the two-nucleon irreducible vertex function in chiral EFT.
- In terms of the $\hat{Q}$ box, the low-energy half-on-shell T matrix of the underlying theory (for a give partial wave) is

$$T(k',k,\,k^2) = \hat{Q}(k',k;\,k^2) + \frac{2}{\pi}\mathcal{P}\int_0^\Lambda \frac{\hat{Q}(k',p;\,k^2)T(p,k;k^2)}{k^2-p^2}\,p^2dp$$

- For two-body scattering in vacuum, the KLR folded diagrams provide a way of re-summing the T-matrix equation in a such a manner that the energy-dependent $\hat{Q}(k',k;\,p^2)$ is replaced by a purely momentum-dependent $V_{\rm lowk}(k',k)$.

$$\Longrightarrow T(k',k,\,k^2) = V_{\rm lowk}(k',k) + \frac{2}{\pi}\mathcal{P}\int_0^\Lambda \frac{V_{\rm lowk}(k',p)\,T(p,k;k^2)}{k^2-p^2}\,p^2dp$$

- Since $\hat{Q} \to V_{\rm lowk}$ preserves the half-on-shell T matrix, we can demand
  $dT(k', k, k^2)/d\Lambda = 0$
  $\Longrightarrow$
  $$\frac{d}{d\Lambda} V_{\rm lowk}(k', k) = \frac{2}{\pi} \frac{V_{\rm lowk}(k', \Lambda)\, T(\Lambda, k; \Lambda^2)}{1 - (k/\Lambda)^2}$$

- Given an initial theory at large Λ, one can construct a physically equivalent effective theory at smaller Λ by integrating the above equation.
- V_{lowk} is found to be essentially independent of the underlying V, insofar as V is fitted to the empirical phase shifts, and the cutoff Λ is chosen around 2 fm^{-1}.
  $\leftrightarrow$ V_{lowk} is model-independent.
- V_{lowk} does not introduce violent short-range correlations into nuclear wave functions, because the high-momentum components have been integrated out by means of the unitary transformation U.
  $\leftrightarrow$ Mean-field calculations already lead to reasonable results, with corrections beyond mean-field approximation being small.

How about the saturation property ? — A big problem !

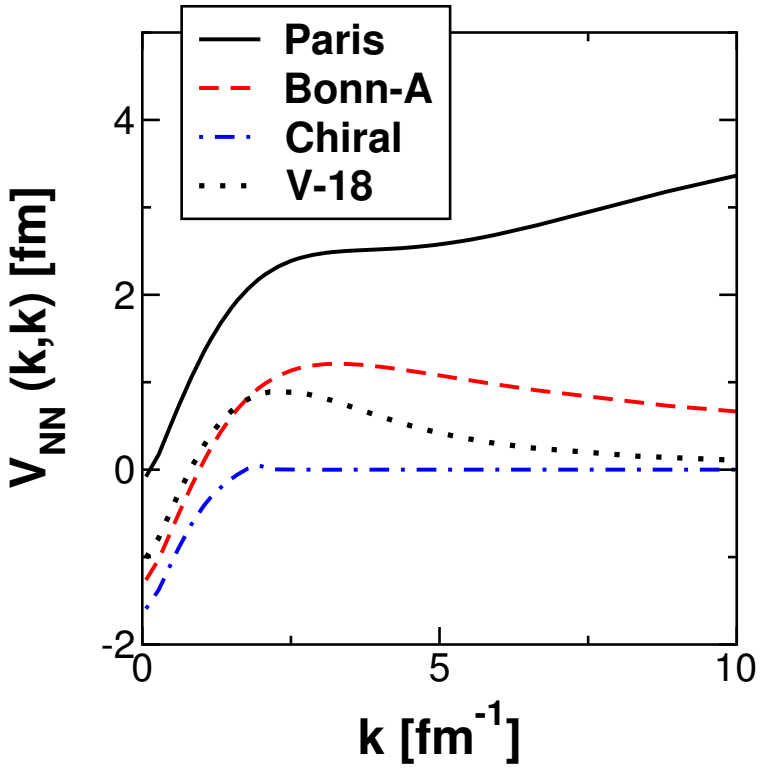

Figure: Diagonal elements of V_{NN} for different bare potentials in the $^1S_0$ channel.

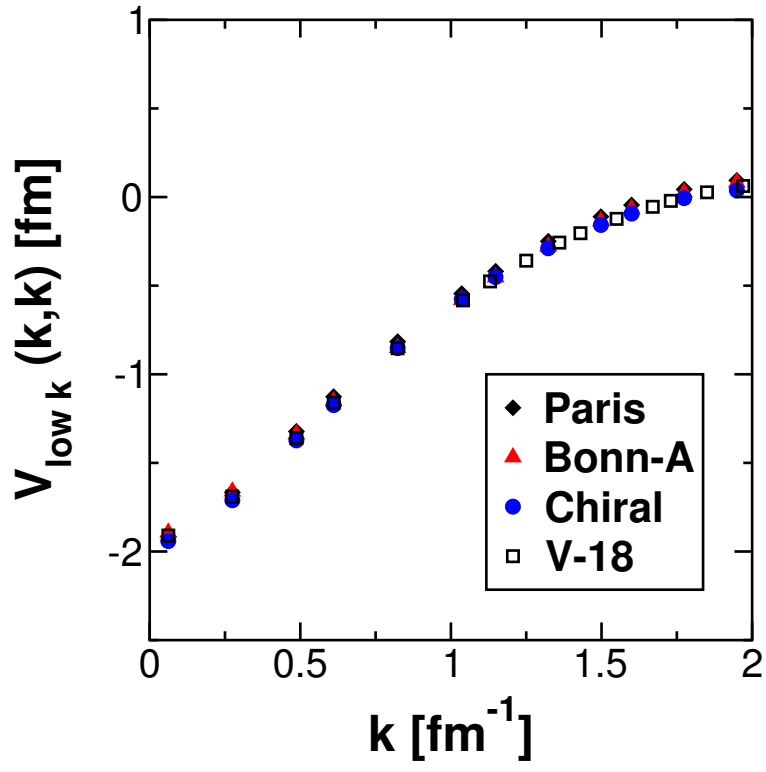

Figure: Diagonal elements of $V_{\mathrm{low\ k}}$ for different bare potentials in the $^1S_0$ channel at a cutoff $\Lambda = 2.0$ fm^{-1}.

Bogner, Kuo, Schwenk, Entem, Machleidt, Phys. Lett. B 576 265-272 (2003)

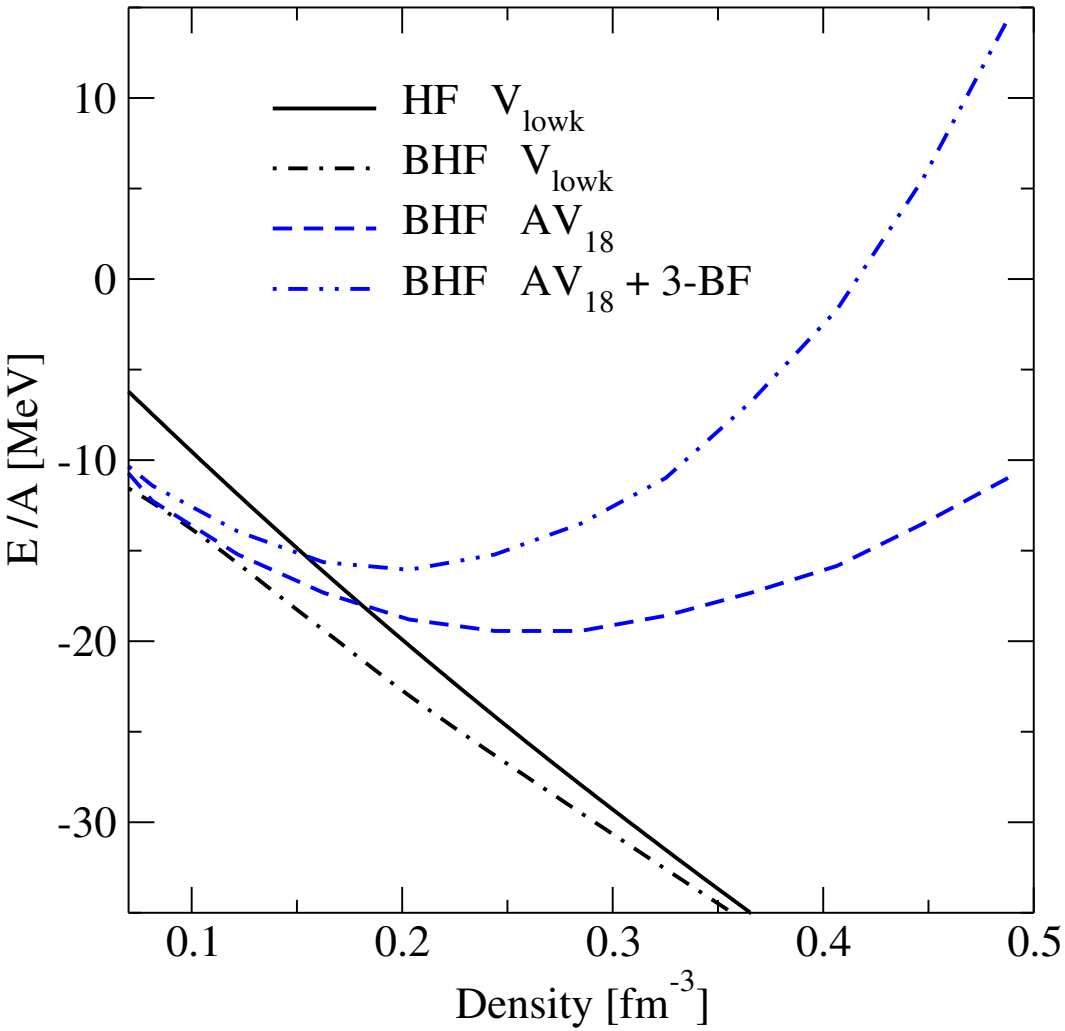

Figure: Binding energy per nucleon of symmetric nuclear matter of a HF calculation (solid line) and of a BHF calculation (dashed dotted line) employing a V_{lowk} interaction are plotted. In addition, the binding energy per nucleon of a nonrelativistic BHF with three-body force calculations (dashed double dotted line) and without three-body force (dashed line) is presented using the Argonne V_{18} potential.

van Dalen and Müther, arXiv:1004.0144 (2010)

Brueckner-Goldstone approach to nuclear matter

—— Linked cluster perturbation series for the ground-state energy of a many-body system

$$
\begin{aligned}
H &= \sum_{i=1}^{A} T_i + \sum_{i<j}^{A} v_{ij} = H_0 + H_1 \\
H_0 &= \sum_{i=1}^{A} (T_i + U_i)\,, \qquad H_1 = \sum_{i<j}^{A} v_{ij} - \sum_{i=1}^{A} U_i
\end{aligned}
$$

- U_i is a one-body potential intended to improve convergence.
- In atomic physics, U_i would be the Hartree-Fock potential.
- Construct a *non-degenerate* Fermi sea from single particle orbits, ϕ_p's:

$$
\begin{aligned}
(T_i + U_i)\phi_p(\vec{r}_i) &= E_p \phi_p(\vec{r}_i) \\
\Phi_0 &= (A!)^{-1/2} \mathcal{A}\left[\, \phi_1(\vec{r}_1) \ldots \phi_A(\vec{r}_A) \,\right] \\
H_0 \Phi_0 &= \mathcal{E}_0 \Phi_0\,, \qquad \mathcal{E}_0 = \sum_{n=1}^{A} E_n
\end{aligned}
$$

For $H\psi = \mathcal{E}\psi$, we have

$$\begin{aligned}
\mathcal{E} &= \mathcal{E}_0 + <\Phi_0|H_1|\Phi_0> + <\Phi_0|H_1(\mathcal{E}_0 - H_0)^{-1}PH_1|\Phi_0> \\
&\quad + <\Phi_0|H_1(\mathcal{E}_0 - H_0)^{-1}PH_1(\mathcal{E}_0 - H_0)^{-1}PH_1|\Phi)> + \ldots \\
&\quad - <\Phi_0|H_0|\Phi_0><\Phi_0|H_1(\mathcal{E}_0 - H_0)^{-2}PH_1|\Phi_0> \ldots \\
P &\equiv 1 - |\Phi_0><\Phi_0|
\end{aligned}$$

• Feynman diagrams in terms of particles and holes defined in reference to the "vacuum" $\Phi_0 \longrightarrow$ Goldstone diagrams

• Only linked diagrams should be retained — Linked diagram expansion

Disconnected diagrams blow up faster than A — disaster

• Goldstone expansion: $\mathcal{E} = \mathcal{E}_0 +$ sum of all connected diagrams

First-order contribution:

$$\mathcal{E}_1 = \frac{1}{2}\sum_{m,n\leq A}(<mn|v|mn> - <mn|v|nm>) - \sum_{n\leq A}<n|U|n>$$

Up to first order

$$\begin{aligned}
\mathcal{E}_{0+1} &\equiv \mathcal{E}_0 + \mathcal{E}_1 \\
&= \sum_{n\leq A}<n|T|n> + \frac{1}{2}\sum_{m,n\leq A}(<mn|v|mn> - <mn|v|nm>)
\end{aligned}$$

Brueckner's reaction matrix — G-matrix

- Nuclear interactions (in H_1) are too singular to be treated in perturbation theory
- Recall that, in free space, even if v is singular, the scattering T defined by

$$T = v + vG_0T \qquad (G_0 = \text{free particle Green's function})$$

  has non-singular behavior.
  (*cf.*, Watson expansion in terms of t (instead of v) for pi-nucleus optical potential)
  However, a Hartree-Fock calculation in terms of T (instead of v) does *not* lead to a stable ground state.
- Need to consider medium effects in carrying out partial summation corresponding to $v \rightarrow T$.
  $\Longrightarrow$ Brueckner G-matrix

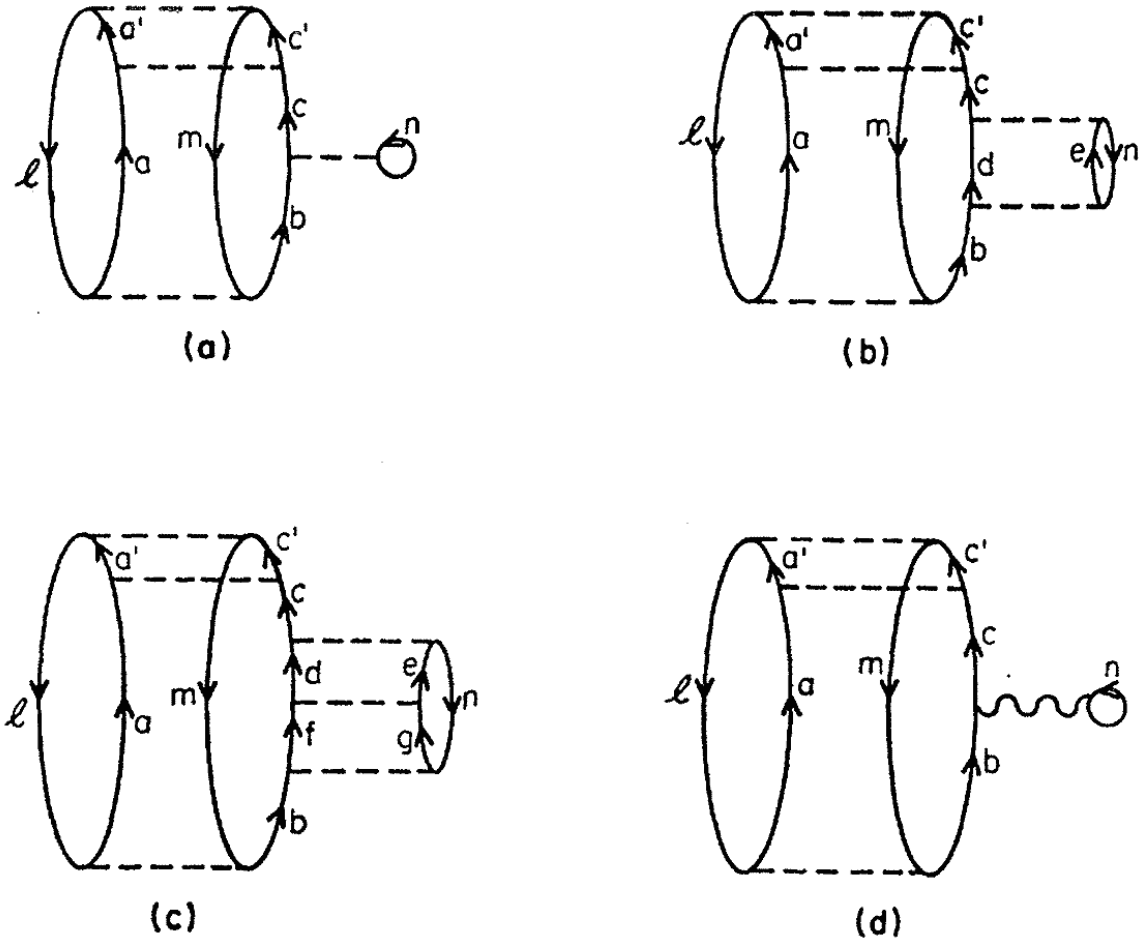

FIG. 10. Diagrams illustrating the summation of ladder diagrams to obtain the G matrix. Diagrams 10(a), (b), (c) are the first three members of an infinite sequence of ladder diagrams whose sum is diagram 10(d), in which the wiggly line represents the G matrix.

B. D. Day, Rev. Mod. Phys. 39, 719-744 (1967)

- Define an in-medium reaction matrix, called the G-matrix, by

$$
\begin{aligned}
G(W) &= v - v(Q/e)G(W) \\
&= v - v(Q/e) + v(Q/e)v(Q/e)v - + \ldots \\
Q|pq> &= \begin{cases} |pq> & \text{if } p > A \text{ and } q > A \\ 0 & \text{otherwise} \end{cases} \\
e\,|pq> &= (E_p + E_q - W)\,|pq>\,,
\end{aligned}
$$

where $|pq>$ stands for $\phi_p(\vec{r}_1)\phi_q(\vec{r}_2)$.

- W is the *starting energy* to be explained below
- $G(W)$ sums up all ladder diagrams for a given pair of two particle lines that occur in a (in general) larger diagram.
- The starting energy W depends on what particle and hole states we start from to build up particle-particle scattering ladders.
- After this partial summation, expansion in H_1, i.e., in v and U, is changed into expansion in G and U.

• Hartree-Fock choice of the single-particle potential U:

$$<p|U|p> \equiv \sum_{k}^{k_F} \{<pk|v|pk> - <pk|v|kp>\} \qquad \text{for } p < k_F$$

• Hartree-Fock ground state energy

$$\mathcal{E}_{0+1} = \sum_{n \leq A} <n|T|n> + \frac{1}{2} \sum_{m,n \leq A} (<mn|v|mn> - <mn|v|nm>)$$

• The Hartree-Fock choice ensures that $\mathcal{E}_{0+1}$ is stationary with respect to variation of the single-particle wave functions
$\longrightarrow$ **Brueckner-Hartree-Fock (BHF) choice of** U

$$\begin{aligned} <p|U|p> &\equiv \sum_{k}^{k_F} \{<pk|G(W)|pk> - <pk|G(W)|kp>\} \qquad \text{for } p < k_F \\ W &= E_p + E_k \end{aligned}$$

Brueckner-Hartree-Fock (BHF) ground-state energy

$$\mathcal{E}_{\mathrm{BHF}} = \sum_{n \leq A} <n|T|n> + \frac{1}{2} \sum_{m,n \leq A} (<mn|G|mn> - <mn|G|nm>)$$

- Can we consider expansion in G and interpret $\mathcal{E}_{\mathrm{BHF}}$ as the 0-th and 1st order terms in this expansion ?
- The answer is NO.
- Addition of one G to a given diagram does *not* lead to a smaller contribution (Bethe 1965)
  $\longrightarrow$ no expansion in G
  $\longrightarrow$ hole-line expansion

Hole-line expansion

- Insertion of a particle line comes with $\int_{k_F}^{\infty} d^3k$ — large phase space
- Insertion of a hole line is accompanied with $\int_0^{k_F} d^3k$ — small phase space
- Diagrams with n_h hole lines scale like κ^{n_h}, where

$$\kappa \equiv 3\,(c/r_0)^3 = 0.14 \qquad (\kappa \propto \rho)$$

$r_0 = 1.12$ fm (inter-nucleon distance); $c = 0.4$ fm (hard core radius)

- $n_h = 2$ terms $\leftrightarrow$ Brueckner-Hartree-Fock term

$$\frac{(\text{potential energy})_{n_h=2}}{A} = -35 \text{ MeV} \tag{5}$$

- $n_h = 3$ terms with all possible G insertions need to be treated as a whole set !
  $\longrightarrow$ Bethe-Faddeev equation

$$\frac{(\text{potential energy})_{n_h=3}}{A} = -5 \text{ MeV} \tag{6}$$

- Indication of convergence

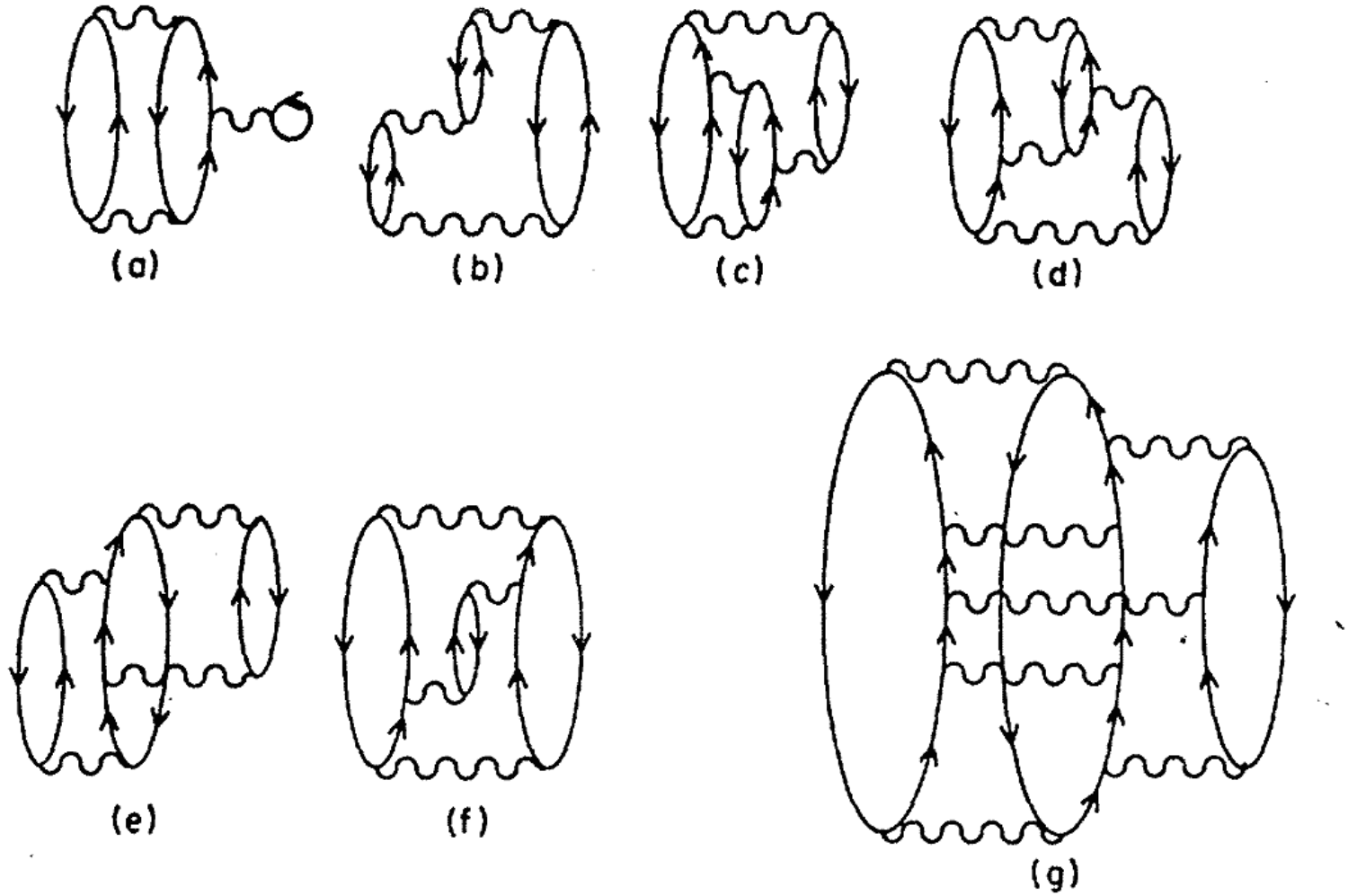

FIG. 33. Some of the three-hole-line diagrams studied by Bethe, as explained in the text.

B. D. Day, Rev. Mod. Phys. 39, 719-744 (1967)

The Coester-band problem

- If we carry out BHF calculations for various high-precision phenomenological potentials, the results (binding energy and saturation density) fall into a band in the BE-ρ plot (so-called the Coester band).
- The Coester band does *not* pass through the empirical point.
- Soft NN interactions tend to produce BE/nucleon tha is close to or below the empirical value, -16 MeV, but at a saturation density larger than $\rho_0^{\rm emp}$ by a factor of 2 or more.
- Stiffer NN interactions (with larger tensor components) may give the correct saturation density but yield BE/nucleon $\approx$ -10 MeV.

  $\Longleftrightarrow$ Coester-line problem [Coester et al., PRC 1 (1970) 769]

  Was a great challenge for many years

Attempts to go beyond the original BHF

- Inclusion of hole-hole ladder diagrams in the reaction matrix [Frick and Muether, 2003]
  — No significant changes in the calculated saturation properties
- Detailed numerical studies of the Bethe-Fadeev equation [Song et al., 1998]
  — Small effects on the Coester band problem

Other many-body techniques

- Coupled cluster method
  [Kümmel, Lührmann and Zabolitzky, 1978; Mihaila and Heisenberg, 2000]
- Variational method incorporating correlated basis functions
  [Bisconti et al., 2006]
- Quantum Monte Carlo calculations
  [Pieper 2001]

The Coester band problem still remains unsolved (within the use of non-relativisitc two-body NN interactions).

Possible way out

(a) Introduction of a phenomenological three-nucleon (3N) forces in a variational calculation reproduces the empirical saturation point — [Friedman and Pandharipande, 1981]
In the BHF context, Fadeev equations including 3N forces need to be solved

(yet to be done ?)

(b) Relativistic effects:

- The self-energy has two components that transform differently under Lorentz transformations
- Interplay between the scalar and vector components can change the saturation properties towards the empirical values.

Variational Monte Carlo (VMC) for nuclear matter

- Variational wave function

$$\Psi = \left(\mathcal{S} \prod_{i<j} \mathcal{F}_{ij} \right) \Phi$$

Φ = Fermi gas wave function
The pair correlation operator, $\mathcal{F}_{ij}$, is parameterized as

$$\begin{aligned} \mathcal{F}_{ij} &= \sum_{p=1}^{8} \beta_p \, f^p(r_{ij}; d_p, \alpha_p) O_{ij}^p \\ O_{ij}^{p=1,8} &= 1, \, \vec{\tau}_i \cdot \vec{\tau}_j, \, \vec{\sigma}_i \cdot \vec{\sigma}_j, \, \vec{\tau}_i \cdot \vec{\tau}_j \, \vec{\sigma}_i \cdot \vec{\sigma}_j, \, S_{ij}, \, S_{ij} \vec{\tau}_i \cdot \vec{\tau}_j, \, \vec{L} \cdot \vec{S}, \, \vec{L} \cdot \vec{S} \, \vec{\tau}_i \cdot \vec{\tau}_j \end{aligned}$$

f^p is a correlation function of the Jastrow type

- When V_{3N} is introduced, a three-body correlation operator might become relevant. An approximate way to simulate this effect is to allow β^p differ from unity.
- Elaborate techniques to calculate the exepctation value of V_{3N} [Meyer diagrams, Fermihypernetted chain (FHNS), single-operator chain (SOC)]

Numerical Results

- Saturation Properties

  With v_{14} alone:

  $$\longrightarrow k_F = 1.8 \text{ fm}^{-1}, \quad \mathcal{E}/A = -20 \text{ MeV}$$

  With $v_{14} + V_{3N}(\text{Tucson})$:

  $$\longrightarrow k_F = 1.8 \text{ fm}^{-1}, \quad \mathcal{E}/A = -24 \text{ MeV}$$

  With $v_{14} + V_{3N}(\text{Type V})$:

  $$\longrightarrow k_F = 1.4 \text{ fm}^{-1}, \quad \mathcal{E}/A = -14.4 \text{ MeV}$$

  Empirical values:

  $$\longrightarrow k_F = 1.42 \text{ fm}^{-1.33}, \quad \mathcal{E}/A = -16 \text{ MeV}$$

  V_{3N} influences the saturation properties significantly

- Compressibility

  With $v_{14} + V_{3N}(\text{Type V})$, $K_{\text{calc.}} = 170$ MeV $\longleftrightarrow$ $K_{\text{empirical}} = 230 \pm 20$ MeV

Saturation property with V_{lowk}

- HF calculation with V_{lowk} for nuclear matter — van Dalen and Muether (2009)
  $\mathcal{E}/A$ in a HF calculation with V_{lowk} goes down *linearly* with ρ.
  $\leftrightarrow$ No saturation at all !
  (HF calculations with V_{lowk} for finite nuclei lead to highly compressed nuclei, if variational space is not constrained, van Dalen et al. 2009.)
- Even a Bruecker-HF calculation cannot cure this problem (van Dalen-Muether)
  $\leftrightarrow$ In sharp contrast to (semi-quantitative) success of BHF with conventional realistic NN potentials (with no cutoff introduced)
- This failure indicates that the roles of the high-momentum component in an NN interaction (or short-range correlation effect) in NN scattering in medium are different from those in NN scattering in free space.
- The use of V_{lowk} for nuclear matter fails to take account of this difference. $V_{lowk} \rightarrow V_{lowk}(\rho)$
- An alternative remedy — 3N forces, Bogner et al. NPA 763 (2005) 59.

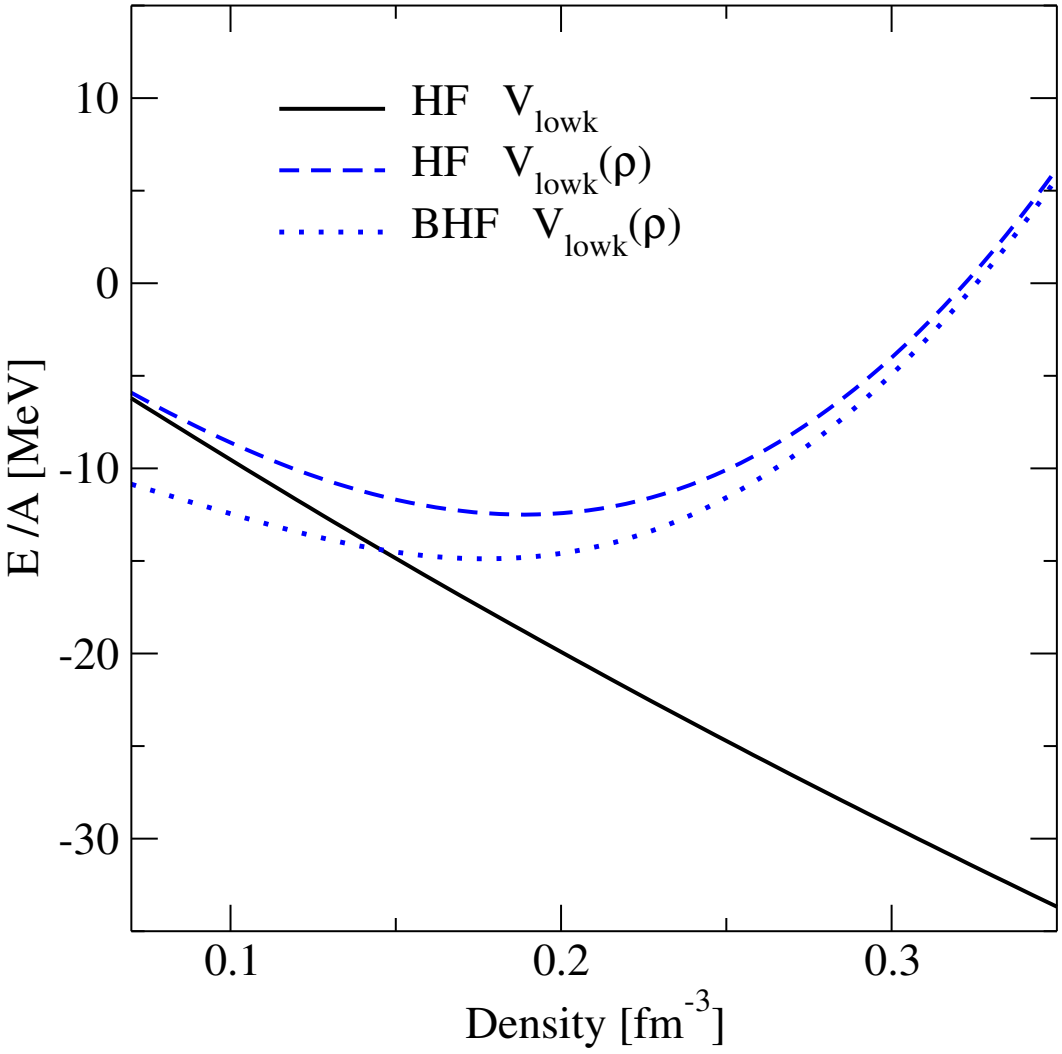

Figure: Binding energy per nucleon of isospin symmetric nuclear matter of a HF calculation (dashed line) and of a BHF calculation (dotted line) employing a density dependent V_{lowk} interaction are plotted. In addition, a HF calculation using a standard V_{lowk} interaction (solid line) is added to the figure.

van Dalen and Müther, arXiv:1004.0144 (2010)

- One way to introduce the ρ-dependence in V_{lowk} is to incorporate relativistic effects

  cf. BHF $\rightarrow$ Dirack-Brueckner-hartree-Fock (DBHF)

  More on the relativisitc effects after explaining the Walecka model

- Procedure to obtain $V_{lowk}(\rho)$

  (i) For a given density, calculate the matrix elements of an underlying realistic NN force for in-medium Dirac spinors (that contain reduced mass effects).

  It is understood that the medium properties are already known from the equation of state obtained with the use of the same underlying NN force.

  (ii) Follow the recipe used in deriving V_{NN} from V_{lowk} for a free-space NN intereaction.

- A HF calculation with $V_{lowk}(\rho)$ (Bonn A potential, $\Lambda = 2\mathrm{fm}^{-1}$) leads to saturation:
  $\rho_{\mathrm{equil}} \simeq 0.2\ \mathrm{fm}^{-3}, \quad \mathcal{E}/A \simeq -12$ MeV.

- A BHF calculation

$$G(k', k, \epsilon_k)_{eff} = V_{eff}(k', k) + \int_0^\Lambda q^2 dq\, V_{eff}(k', q)\, \frac{Q_P}{2\epsilon_k - 2\epsilon_q + i\eta}\, G(q, k, \epsilon_k)$$

$$Q_P = \text{Pauli operator}, \quad \epsilon_i = \text{single particle energy} \quad (i = k, q)$$

  BHF gives lowers $\mathcal{E}/A$ by about 2 MeV and gives $\mathcal{E}/A \simeq -14$ MeV at $\rho_{\mathrm{equil}} \simeq 0.18\ \mathrm{fm}^{-3}$. (The minimum is very shallow, however.)

- A nuclear matter calculation based on V_{NN}^{EFT} should show similar "pathology" as V_{lowk}.
  Fixing the LECs in free space (non-relativistically) may miss some medium effects.

Walecka model

Relativistic Mean Field Theory (RMF)

— *cf.* Serot and Walecka, Adv. Nucl. Phys. 16 (1986) 1

- System of (relativistic) nucleons, neutral scalar mesons, and neutral vector mesons

$$\begin{aligned}\mathcal{L}_I &= \bar{\psi}\left[\gamma_\mu(i\partial^\mu - g_v V^\mu) - (M - g_s\phi)\right]\psi \\ &\quad + \frac{1}{2}\left(\partial_\mu\phi\partial^\mu\phi - m_s^2\phi^2\right) - \frac{1}{4}F_{\mu\nu}F^{\mu\nu} + \frac{1}{2}m_v^2 V_\mu V^\mu\,,\end{aligned}$$

  where $F_{\mu\nu} \equiv \partial_\mu V_\nu - \partial_\nu V_\mu$

- In the limit of heavy, static baryons, one-meson exchange gives rise to

$$V_{\text{eff}}(r) = \frac{g_v^2}{4\pi}\frac{e^{-m_v r}}{r} - \frac{g_s^2}{4\pi}\frac{e^{-m_s r}}{r}$$

  Can simulate long-range attraction and short-range repulsion.

- Lagrange equations

$$(\partial_\mu \partial^\mu + m_s^2)\phi = g_s \bar{\psi}\psi$$
$$\partial_\mu F^{\mu\nu} + m_v^2 V^\nu = g_v \bar{\psi}\gamma^\nu \psi$$
$$[\gamma^\mu (i\partial_\mu - g_v V_\mu) - (M - g_v \phi)]\psi = 0$$

- As the baryon density increases, the source terms become large.
  $\rightarrow$ Meson field operators can be replaced by their expectation values:

$$\begin{aligned} \phi &\rightarrow < \phi > \equiv \phi_0 \\ V_\mu &\rightarrow < V_\mu > \equiv \delta_{\mu 0} V_0 \end{aligned}$$

- For a static, uniform system $\leftrightarrow$ ϕ_0 and V_0 are constants
- Rotational invariance $\leftrightarrow$ $< \vec{V} > = 0$

- The equations for the mesons can be solved immediately for constant ϕ_0 and V_0

$$\begin{aligned} \phi_0 &= \frac{g_s}{m_s^2} <\bar{\psi}\psi> \equiv \frac{g_s}{m_s^2}\,\rho_s \qquad (\rho_s = \text{scalar density}) \\ V_0 &= \frac{g_v}{m_v^2} <\psi^\dagger\psi> \equiv \frac{g_v}{m_v^2}\,\rho_B \qquad (\rho_B = \text{baryon density}) \end{aligned}$$

- Equation for ψ becomes

$$[i\gamma_\mu\partial^\mu - g_v\gamma^0 V_0 - (M - g_v\phi_0)]\psi = 0$$

- For $\psi = \psi(\vec{k},\lambda)e^{i\vec{k}\cdot\vec{x}-i\epsilon(k)t}$, we have

$$(\vec{\alpha}\cdot\vec{k} + \beta M^*)\psi(\vec{k},\lambda) = [\epsilon(k) - g_v V_0]\psi(\vec{k},\lambda)\,, \quad M^* \equiv M - g_s\phi_0$$
$$\epsilon(k) \equiv \epsilon^{(\pm)}(k) = g_v V_0 \pm (\vec{k}^2 + M^{*2})^{1/2} \equiv g_v V_0 \pm E^*(k)$$

- ϕ_0 changes the nucleon mass; V_0 changes the nucleon frequency (energy)

- We can introduce the quantization of ψ in much the same way as for a free Dirac field
  $\rightarrow$ Effective Hamiltonian

$$\hat{H} - <0|\hat{H}|0> = \hat{H}_{\rm MFT} + \delta H$$

$$\hat{H}_{\rm MFT} = \sum_{\vec{k}\lambda} (\vec{k}^2 + M^{*2})^{1/2} (A^\dagger_{\vec{k}\lambda} A_{\vec{k}\lambda} + B^\dagger_{\vec{k}\lambda} B_{\vec{k}\lambda})$$

$$+ g_v V_0 \hat{B} - V(\frac{1}{2} m_v^2 V_0^2 - \frac{1}{2} m_s^2 \phi_0^2)$$

$$\delta H = -\sum_{\vec{k}\lambda} [(\vec{k}^2 + M^{*2})^{1/2} - (\vec{k}^2 + M^2)^{1/2}]$$

with $\hat{B} = \sum_{\vec{k}\lambda} (A^\dagger_{\vec{k}\lambda} A_{\vec{k}\lambda} - B^\dagger_{\vec{k}\lambda} B_{\vec{k}\lambda})$, and V is the volume of the system.

Nuclear matter

- Fill states with wave number $\vec{k}$ and spin-isospin degeneracy $\gamma = 4$ up to k_F.

$$\rho_B = \frac{\gamma}{(2\pi)^3} \int_0^{k_F} d^3k = \frac{\gamma}{6\pi^2} k_F^3$$

$$\mathcal{E} = \frac{g_v^2}{2m_v^2} \rho_B^2 + \frac{m_s^2}{2g_s^2} (M - M^*)^2 + \frac{\gamma}{(2\pi)^3} \int_0^{k_f} d^3k \, (\vec{k}^2 + M^{*2})^{1/2}$$

- $\rho_B = B/V$ is a given number
  $\longrightarrow$ $M^*{=}M - g_s\phi_0$ is the only quantity to be determined by solving dynamics.
  $\longrightarrow$ Minimize $\mathcal{E}(M^*)$ with respect to M^*.
  $\longrightarrow$ Self-cosistency relation

$$\begin{aligned} M^* &= M - \frac{g_s^2}{m_s^2}\frac{\gamma}{(2\pi)^3}\int_0^{k_F} d^3k\,\frac{M^*}{(\vec{k}^2 + M^{*2})^{1/2}} \\ &= M - \frac{g_s^2}{m_s^2}\frac{\gamma M^*}{4\pi^2}\left[k_F E_F^* - M^{*2}\ln\left(\frac{\mathrm{k_F} + \mathrm{E_F^*}}{\mathrm{M^*}}\right)\right] \end{aligned}$$

$$E_F^* \equiv (k_F^2 + M^{*2})^{1/2}$$

- High-density limit: $k_F \to \infty$

$$\mathcal{E} \longrightarrow \rho_B\left[\frac{g_v^2}{2m_V^2}\rho_B + \frac{3}{4}k_F + \frac{m_s^2 M^2}{2g_s^2\rho_B} + O(\rho_B^{-5/3})\right]$$

- In both limits, the system is unbound ($E/B > M$)
  $\longrightarrow$ The system saturates (if the scalar-meson attraction is strong enough).

Phenomenological choice of parameters

Use the empirical equilibirum properties:

$$\left(\frac{E-BM}{B}\right)_0 = -15.75\,\mathrm{MeV}\,, \quad k_F^0 = 1.42\ \mathrm{fm}^{-1}\ (\gamma = 4)$$

$$\Rightarrow C_s^2 \equiv g_s^2\,(M^2/m_s^2) = 267.1\,, \quad C_V^2 \equiv g_v^2\,(M^2/m_v^2) = 195.9$$

- M^*/M decreases significantly as k_F augments
  $M^*/M \approx 0.5$ at ordinary nuclear density
  due to the large condensed scalar field $g_s\phi_0 \approx 400MeV$
- Large $g_s\phi_0 \rightarrow$ huge attractive contribution to E/B
- Large repulsive E/B from the vector field $g_vV_0 \approx 330$ MeV
- Lorentz structure of the interaction leads to a new energy scale
  Small binding energy ($\approx$ 16 MeV)
  $\leftrightarrow$ Cancellation between the large scalar attraction and vector repulsion

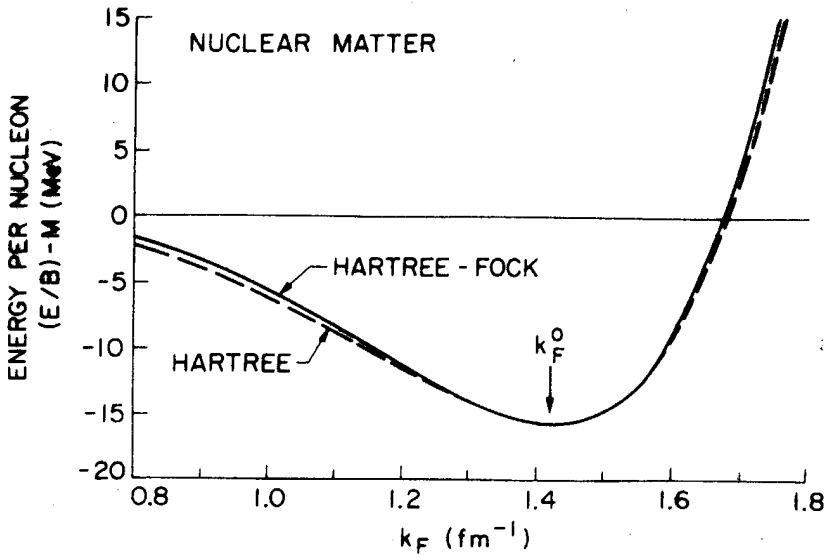

Figure: Energy/nucleon in nuclear matter. The MFT (Hartree) and HF (Hartree-Fock) results here use the MFT (QHD-I) and HF coupling constants chosen to reproduce the saturation properties of nuclear matter at the minimum of these curves. Serot, Walecka, Adv. Nucl. Phys. 16 (1986) 1.

- The change $M \to M^*$ enhances the lower component of in-medium Dirac spinors.
  Sharp rise in incompressibility for large k_F.
- Hartree-Fock estimates based on the *"potential"* limit

$$V_{\rm eff}(r) = \frac{g_v^2}{4\pi}\frac{e^{-m_v r}}{r} - \frac{g_s^2}{4\pi}\frac{e^{-m_s r}}{r}$$

leads to collapse of nuclear matter as k_F increases !

Prediction for neutron matter ($\gamma = 2$):

- Shallow minimum around $k_F = 1.4\,\mathrm{fm}^{-1}$ (but unbound)

Predictions for other properties ← RMF contains only two parameters

- Symmetry energy coefficient:
  $b_{\mathrm{sym}}^{\mathrm{calc}} = 22.1$ MeV
  $b_{\mathrm{sym}}^{\mathrm{emp}} = 33.2$ MeV [Seeger and Howard, NPA 238 (1975) 491].
- Effective nucleon mass:
  $(M^*/M)^{\mathrm{calc}} = 0.56$
  $(M^*/M)^{\mathrm{emp}} \approx 0.6$ [Bethe, Ann. Rev. Nucl. Sci.21 (1971) 125]
- Compressibility:
  $(K)^{\mathrm{calc}} = 540$ MeV
  $(K)^{\mathrm{emp}} = 200$-300 MeV
- Meson coupling constants:
  $(C_s^2)^{\mathrm{calc}} = 267\,,\ (C_v^2)^{\mathrm{calc}} = 196$
  $(C_s^2)^{\mathrm{emp}} \approx 300\,,\ (C_v^2)^{\mathrm{calc}} \approx 310$ [Brayan and Scott, Phys. Rev. 177 (1969) 1435]

Properties of finite nuclei

- $\phi_0 \rightarrow \phi(r)$ and $V_0 \rightarrow V_0(r)$
- Inclusion of ρ meson for $Z \neq N$ nuclei
- Inclusion of Coulomb force
  $\rightarrow$ Predictions for matter and charge distributions in finite nuclei

Proton-nucleus scattering at intermediate energies (E_p = 500-800 MeV).

- Invariant N-N scattering amplitude

$$\mathcal{T} = \mathcal{T}_S + \mathcal{T}_V \gamma^{\mu}_{(1)} \gamma_{\mu(2)} + \mathcal{T}_P \gamma^5_{(1)} \gamma^5_{(2)} + \mathcal{T}_A \gamma^5_{(1)} \gamma^{\mu}_{(1)} \gamma^5_{(2)} \gamma_{(2)\mu} + \mathcal{T}_T \sigma^{\mu\nu}_{(1)} \sigma_{\mu\nu(2)}$$

- Boost this amplitude from the N-N system to N-nucleus system.
- Construct an optical potential in relativistic impulse approximation.

$$U_{\rm opt}(q, T_L) = \frac{-4i\pi k_c}{M} < \underline{F} | \sum_{i=1}^{A} e^{i\vec{q}\cdot\vec{x}_{(i)}} \mathcal{T}(t,s) | \underline{F} >$$

where $|\underline{F}>$ is the target ground state in RMFT.

Proton scattering from a spin-zero target

$$T(\theta) = g(\theta) + h(\theta)\sigma \cdot \hat{n}$$

- Three observables — Differential cross sections (σ), Polarization or analyzing power (P), and spin-rotation function (Q)

$$\begin{aligned} \sigma &= |g|^2 + |h|^2 \\ P &= 2Re(g^* h)/(|g|^2 + |h|^2) \\ Q &= 2Im(gh^*)/(|g|^2 + |h|^2) \end{aligned}$$

- Comparison of with data (e.g., p+^{208}Pb at 800 MeV)
- Calculation [Clark et al., PRL, 50 (1983)1644]
  - σ agrees with data and with non-relativistic calculations
  - P and Q agree very well with data
    — dramatic improvement over non-relativistic approaches !

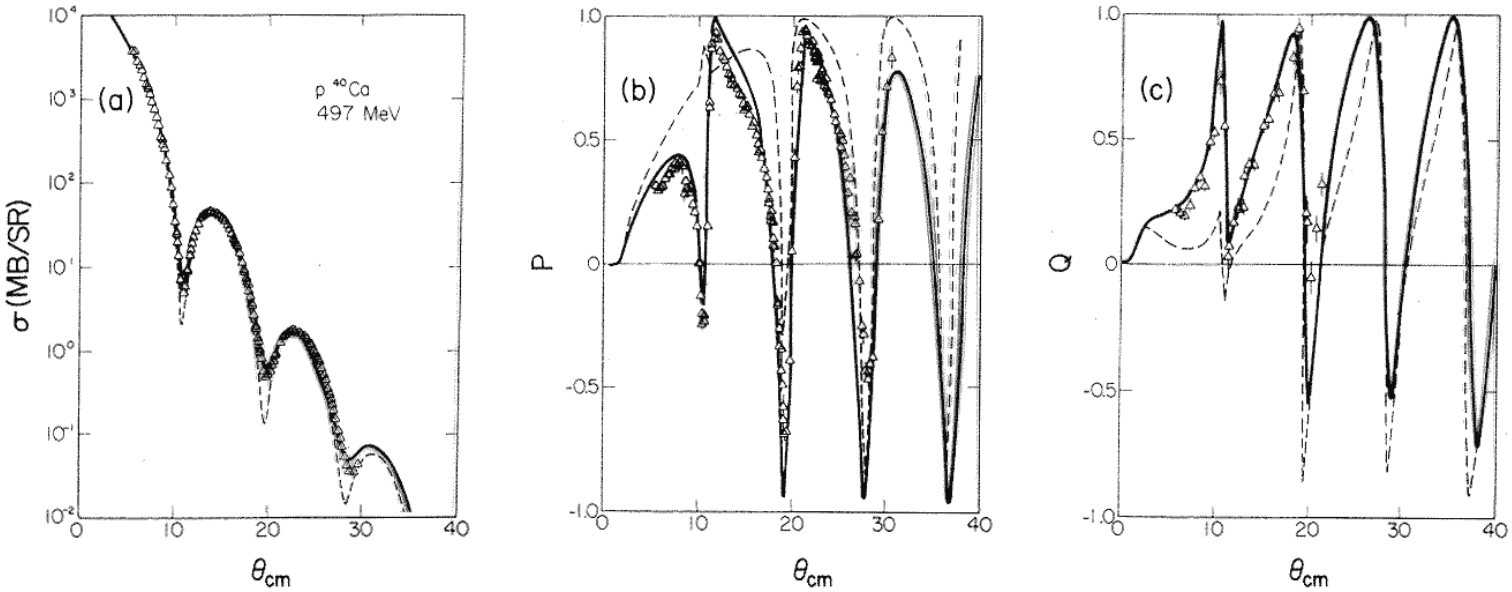

Figure: Calculated cross section (a), analyzing power (b), and spin-rotation function (c) for $p+^{40}$Ca at $T_L = 497\mathrm{MeV}$ using the Dirac impulse approximation (RIA, solid curve) and the nonrelativistic impulse approximation (NRIA, dashed curve).

Serot, Walecka, Adv. Nucl. Phys. 16 (1986) 1.

Beyond Mean-Field Approximation — Quantum Hadrodynamics (QHD)

- For the lagrangian $\mathcal{L}^I$, and for a given non-interacting Fermi sea, we can derive Feynman rules.
- Treatment of the nucleon propagator

$$iG^0_{\alpha\beta}(x'-x) = <\Psi_0|T[\psi_\alpha(x')\bar{\psi}_\beta(x)]|\Psi_0> = i\int \frac{d^4k}{(2\pi)^4} e^{-ik\cdot(x'-x)} G^0_{\alpha\beta}(k)$$

where $|\Psi_0>$ is the non-interacting ground state (Fermi sea), and the fields are in the interaction picture.

$$\begin{aligned} G^0_{\alpha\beta}(k)| &= \frac{\theta(k_0 - E^0(k_F))}{\not{k} - M + i\epsilon} + \frac{\theta(E^0(k_F) - k_0)}{\not{k} - M - i\epsilon} \\ &= (\gamma_\mu k^\mu + M)_{\alpha\beta}\left[\frac{1}{k^2 - M^2 + i\epsilon} + \frac{i\pi}{E^0(k)}\delta(k^0 - E^0(k))\theta(k_F - |\vec{k}|)\right] \\ &\equiv G^0_F(k)_{\alpha\beta} + G^0_D(k)_{\alpha\beta} \quad \text{with } E^0(k) = (\vec{k}^2 + M^2)^{1/2} \end{aligned}$$

- Full propagator

$$iG_{\alpha\beta}(x'-x) = <\Psi|T[\psi_{H\alpha}(x')\bar{\psi}_{H\beta}(x)]|\Psi>$$

where $|\Psi>$ is the interacting ground state, and the fields are Heisenberg fields.

- Energy density in the relativistic Hartree approximation (RHA)

$$\begin{aligned}\mathcal{E}_{\rm RHA} &= \frac{g_v^2}{2m_v^2}\,\rho_B^2 + \frac{m_s^2}{2g_s^2}\,(M-M^*)^2 \\ &\qquad + \frac{\gamma}{(2\pi)^3}\int_0^{k_f} d^3k\,(\vec{k}^2+M^{*2})^{1/2} + \Delta\mathcal{E}_{\rm VF} \\ &= \mathcal{E}_{\rm MFT} + \Delta\mathcal{E}_{\rm VF}\end{aligned}$$

- Vacuum fluctuation energy given by

$$\begin{aligned}\Delta\mathcal{E}_{\rm VF} &= -\frac{1}{4\pi^2}\left[M^{*4}\ln\left(\frac{\rm M^*}{\rm M}\right) + {\rm M}^3({\rm M}-{\rm M}^*) - \frac{7}{2}\,{\rm M}^2({\rm M}-{\rm M}^*)^2\right. \\ &\qquad \left. + \frac{13}{3}M(M-M^*)^3 - \frac{25}{12}\,(M-M*)^4\right]\end{aligned}$$

Relativistic Hartree-Fock approach

- Exchange corrections included
  $\longrightarrow$ Pions can come into the picture

$$
\begin{aligned}
\mathcal{E} \;=\; & \frac{\gamma}{(2\pi)^3}\int_0^{k_F} d^3k E(k) + \frac{g_s^2}{2m_s^2}\rho_s^2 - \frac{g_v^2}{2m_v^2}\rho_B^2 \\
& + \frac{1}{2}\,\frac{\gamma}{(2\pi)^3}\int_0^{k_F}\frac{d^3k}{E^*(k)}\int_0^{k_F}\frac{d^3q}{E^*(q)} \\
& \times\left\{ g_s^2 D_s^0(k-q)\left[\frac{1}{2} - [E(k)-E(q)]^2 D_s^0(k-q)\right]\right. \\
& \times [k^{*\mu}q^*_\mu + M^*(k)M^*(q)] + 2g_v^2 D_v^0(k-q) \\
& \left.\times\left[\frac{1}{2} - [E(k)-E(q)]^2 D_V^0(k-q)\right][k^{*\mu}q^*_\mu - 2M^*(k)M^*(q)]\right\}
\end{aligned}
$$

$$
\begin{aligned}
M^*(k) &\equiv M + \Sigma^s(k)\,, \quad \vec{k}^* \equiv \vec{k}[1+\Sigma^v(k)] \\
E^*(k) &\equiv [\vec{k}^{*2} + M^{*2}(k)]^{1/2}\,, \quad k^{*\mu} \equiv k^\mu + \Sigma^\mu(k)
\end{aligned}
$$

- If the parameters are readjusted to reproduce b_v and k_F, the results of RHFA are similar to those of RHA (apart from the single-particle spectrum).
  $\Rightarrow$ Compressibility too high as compared with the empirical value !

Relativistic Brueckner-Hartree-Fock

Relativistic extension of the Brueckner-Hartree-Fock (BHF)
$\rightarrow$ Dirac-Brueckner-Hartree-Fock (DBHF)

— Anastasio et al., Phys. Rep. 100 (1983) 327;
— ter Haar and Malfliert, Phys. Rep. 149 (1987) 207;
— Horowitz and Serot, NPA, 464 (1987) 613;
— Machleidt, Adv. Nucl. Phys. 19 (1989), etc.

- Start with the Bethe-Salpeter equation for NN-scattering

$$\langle p|T|p'\rangle = \langle p|K|p'\rangle + i\int \frac{d^4p''}{(2\pi)^4}\langle p|K|p''\rangle G(p'')G(-p'')\langle p''|T|p''\rangle$$

$$K = \text{full two-body kernel}, \quad G(p) = \text{Feynman propagator}$$

Major approximation (in the spirit of NN forces):
— Take as the kernel K one-boson exchange tree diagrams.
$\longrightarrow$ Relativistic ladder diagrams (relativistic G-matrices)

- Three-dimensional reduction

$$T = V + Vg_2T$$
$$V = K + K(GG - g_2)V$$

Each choice of the two-body propagator $g_2 \leftrightarrow$ specific form of the quasi-potential

- Thompson equation [PRD 1 (1970) 110]

$$g_2(\bar{p}) = -i \int dp_0 G(p) G(-p)$$

Approximate V as

$$\begin{aligned} <\bar{p}, -\bar{p}|V|\bar{p}', -\bar{p}'> &= <(\frac{\sqrt{s}}{2}, \bar{p}), (\frac{\sqrt{s}}{2}, -\bar{p}) \,|\, K \,|\, (\frac{\sqrt{s}}{2}, \bar{p}'), (\frac{\sqrt{s}}{2}, -\bar{p}')> \\ s &= \text{invariant mass of the two}-\text{body system} \end{aligned}$$

- In $g_2(\bar{p}) = -i \int dp_0 G(p) G(-p)$, retain only positive energy states:

$$G(p) \to \frac{m}{E_p} \frac{\Lambda^+}{p_0 - E_p}$$

This approximation leads to

$$g_2(p, s) = \Lambda^+(\bar{p}) \Lambda^+(-\bar{p}) \frac{m^2}{E_p^2} \frac{\pi}{\sqrt{s}/2 - E_p + i\epsilon}$$

- The scattering equation becomes

$$\begin{aligned} <\bar{p}|T(s)|\bar{p}'> &= <\bar{p}|V|\bar{p}'> + \int \frac{dp''}{(2\pi)^3} <\bar{p}|V|\bar{p}''> \\ &\quad \times \frac{m^2}{2E_p^2} \frac{1}{\sqrt{s}/2 - E_{p''} + i\epsilon} < \bar{p}''|T(s)|\bar{p}'> \end{aligned}$$

Choice of one-boson exchange diagrams

- Take six mesons: π, ρ, ω, ϵ, η and δ mesons
- Some of them (e.g., π, ω) correspond to physical particles (with known masses and coupling constants)
- Others mimic processes not included in the one-boson exchange with physical mesons;
  ϵ (δ) simulates the isoscalar (isovector) part of multi-pion exchanges.

$$\begin{aligned}\mathcal{L} &= -g_{\epsilon,\delta}\bar{\psi}\psi\phi_{\epsilon,\delta} - ig_{\pi,\eta}\bar{\psi}\frac{\gamma^5\gamma^\mu}{2m_N}\psi(\partial_\mu\phi_{\pi,\eta}) \\ &\quad -g_{\omega,\rho}\bar{\psi}\gamma_\mu\psi\phi^\mu_{\omega,\rho} - i\,f_{\omega,\rho}\frac{\sigma^{\mu\nu}}{2m_N}\psi(\partial_\mu\phi^{\omega,\rho}_\nu)\end{aligned}$$

Each vertex carrying a form factor $\Lambda^2/(\Lambda^2+k^2)$

- From calculated $<\bar{p}|T(s)|\bar{p}'>$, derive the phase shifts and fit them to the data

Caveat:

- A model that does not treat negative-energy states properly cannot be genuinely relativistic $\leftrightarrow$ "Minimal relativity"
- The term "relativistic" is used here to distinguish this treatment from other nuclear matter calculations that do not take into account the Lorentz structure of the self-energy, or relativistic kinematics.

Relativistic treatment of nuclear matter — DBHF

- In medium the nucleon gets dressed because of its interaction with the other nucleons: $G_0(p) \rightarrow G(p)$.

$$\begin{aligned} G(p) &= G^0(p) + G^0(p)\Sigma(p)G(p) \\ G(p) &= \frac{\theta(p_0 - E(p_f))}{\not{p} - m - \Sigma(p) + i\epsilon} + \frac{\theta(E(p_f) - p_0)}{\not{p} - m - \Sigma(p) - i\epsilon} \end{aligned}$$

- Define Σ à la BHF (instead of G, use T introduced above).

$$\Sigma(p) = -i \int \frac{d^4p'}{(2\pi)^4} Tr\left[G(p')\{<p,p'|T|p,p'> - <p,p'|T|p',p>\}\right]$$

- Decompose Σ into Lorentz components.

$$\Sigma(p) = \Sigma^s(p) - \gamma^0\Sigma^0(p) + \vec{\gamma}\cdot\vec{p}\,\Sigma^v(p)$$

- In-medium effective quantities:
$m^*(p) = m + \Sigma^s(p)\,,\;\; p_0^*(p) = p_0 + \Sigma^0(p)\,,\;\; \vec{p}^*(p) = \vec{p}(1 + \Sigma^v(p))$

- Dressed Dirac equation and corresponding Green's function

$$(\not{p} - m - \Sigma)\psi^*(p) = (\not{p}^* - m^*)\psi^*(p) = 0$$

$$G(p) = \frac{\theta(p_0 - E(p_f))}{\not{p}^* - m^* + i\epsilon} + \frac{\theta(E(p_f) - p_0)}{\not{p}^* - m^* - i\epsilon}$$

DBHF Self-consistency

$$
\begin{aligned}
<\vec{p}|T(s)|\vec{p}'> &= <\vec{p}|V|\vec{p}'> + \int \frac{d\vec{p}''}{(2\pi)^3} <\vec{p}|V|\vec{p}''> \\
&\quad \times \frac{m^{*2}}{2(E^*_{p''})^2} \frac{\bar{Q}(p'', s^*, P)}{(\sqrt{s}^*/2) - E^*_{p''} + i\epsilon} <\vec{p}''|T(s)|\vec{p}'> \\
s^* &= (p^*_1 + p^*_2)^2\,, \quad P = |\vec{p}_1 + \vec{p}_2|
\end{aligned}
$$

- Recall that the asterisked quantities depend on $T(s)$.
- $<\vec{p}|V|\vec{p}'>$ now stands for $\bar{u}^*(\vec{p})\bar{u}^*(-\vec{p})Vu^*(\vec{p}')u^*(-\vec{p}')$.
- In non-relativisitc nuclear matter, the single-particle orbits are always plane waves $\leftrightarrow$ No need for self-consistency in the wave functions
- In finite nuclei, atomic physics, etc., single-particle orbits must be determined self-consistently.
- Likewise, in relativistic theory of nuclear matter, the 4-spinor structure of single-particle orbits reflects the medium effects.

Nuclear matter properties calculated in DBHF

- Binding energy per nucleon

$$\mathcal{E}/A = \frac{1}{\rho}\int_0^{p_F}\frac{dp}{2\pi} < \bar{u}^*(p)|\vec{\gamma}\cdot\vec{p} + m_N + \frac{1}{2}\Sigma\,|u^*(p)> \frac{m^*_{\rm sc}}{E^*_p} - m_N$$

$$m^*_{\rm sc} \equiv \frac{m_N + \Sigma^s}{1+\Sigma^v}$$

- Saturation point:
  Calculated:
  $[p_F]_{\rm RBHF} = 0.28$ GeV$/c$, $[\mathcal{E}/A]_{\rm RBHF}$ = -14.8 MeV
  Empirical values:
  $p_F = 0.27$ GeV$/c$, $\mathcal{E}/A$ = -16 MeV
- Compressibility at the saturation point:
  Calculated value:
  $K_{\rm RBHF} = 250 \pm 30$ MeV
  Empirical value:
  $K = 210 \pm 30$ MeV (Blaizot et al. 1988);
  $K = 300 \pm 25$ MeV from giant monopole resonance (Sharma et al., 1988)

Standard nuclear physics approach (SNPA)

- The phenomenological potential picture — highly successful.
- A-nucleon system described by a Hamiltonian

$$H^{\rm phen} = \sum_{i=1}^{A} t_i \; + \sum_{i<j}^{A} V_{ij}^{\rm phen} + \sum_{i<j<k}^{A} V_{ijk}^{\rm phen} \; ,$$

- Short-distance behavior in V_{ij}^{phen} — model-dependent
  $\leftrightarrow$ Assume a functional form and adjust parameters to reproduce the two-nucleon data.
- *High-precision phenomenological* N-N potential ($\chi^2 \sim 1$):
  AV18, Nijm, CD-Bonn

- Nuclear wave function $|\Psi^{\rm phen}>$:

$$H^{\rm phen}|\Psi^{\rm phen}> = E|\Psi^{\rm phen}> \ .$$

- In general, finding useful truncation schemes for $|\Psi^{\rm phen}>$ is one of the major goals in nuclear physics (shell model, cluster model, RPA, collective model, etc.)
- For lightest nuclei — **exact, or practically exact solutions** available !!
- So far, up to A=12, and the limit is being pushed up rapidly.
  (mostly bound states; scattering states harder to deal with)
  S. Pieper, NPA 751 (2005) 516c.

Quantum Monte Carlo methods

Argonne-Urbana-Champaign group, and others

Variational Monte Carlo (VMC)

VMC finds an upper bound, E_T, to an eigen-energy of H by evaluating the expectation value of H in a trial wave function, Ψ_T.

$$|\Psi_T> = \left[1 + \sum_{i,j,k} U_{ijk}\right] \left[\mathcal{S} \prod_{i<j} (1 + U_{ij})\right] |\Psi_J>$$

- U_{ij} and U_{ijk} — non-commuting two- and three-nucleon correlation operators
  (the most important being the tensor-isospin correlation corresponding to the pion-exchange potential); $\mathcal{S}$ — symmetric sum over all possible orderings
- Ψ_J — fully antisymmetrized Jastrow wave function that determines the quantum numbers of the state under consideration
- Ψ_J for p-shell nuclei starts with a sum of independent-particle terms, Φ_A, that have four nucleons in an α-like core and (A-4) nucleons in p-shell orbitals.
- These orbitals are coupled in a $LS[n]$ basis to obtain the desired JM value; n specifies the spatial symmetry $[n]$ of the p-shell orbitals.

- This independent-particle basis, Φ_A, is acted on by products of central pair and triplet correlation functions:

$$|\Psi_J> = \mathcal{A}\left\{\left[\prod_{i<j<k} f^c_{ijk}\right]\left[\prod_{i<j\leq 4} f_{ss}(r_{ij})\right]\sum_{LS[n]}\left(\beta_{LS[n]}\left[\prod_{k\leq 4<l\leq A} f^{LS[n]}_{sp}(r_{kl})\right]\right.\right.$$
$$\left.\left.\times\left[\prod_{4<l<m\leq A} f^{LS[n]}_{pp}(r_{lm})\right]|\Phi_A(LS[n]JMTT_3)_{1234:5\ldots A}\right)\right\}$$

- $\mathcal{A}$ indicates an antisymmetrized sum over all possible partitions of the A particles into 4 s-shell and (A-4) p-shell ones.

Green's function Monte Carlo (GFMC)

GFMC projects out the lowest-energy ground state from the VMC Ψ_T by using

$$\Psi(\tau) = \mathrm{e}^{-(H_0-E_0)\tau}\Psi_T$$
$$\Psi_0 = \lim_{\tau\to\infty}\Psi(\tau)$$

- If sufficiently large τ is reached, the eigenvalue E_0 is calculated exactly, while other expectation values are generally calculated neglecting terms of order $|\Psi_0 - \Psi_T|^2$ and higher.
- In contrast, the error in the variational energy, E_T is of order $|\Psi_0 - \Psi_T|^2$, and other expectation values calculated with Ψ_T have errors of order $|\Psi_0 - \Psi_T|$.

GFMC Evaluation of Excited States

- It is possible to treat at least a few excited states with the same quantum numbers using VMC and GFMC.
- Prepare $\Psi_{T,i}$ $(i = 1, 2, \ldots)$ with given quantum numbers (J^π, T)
$$< \Psi_{T,i} | \Psi_{T,j} >= 0 \text{ for } i \neq j$$
- Generate the GFMC wave function, $\Psi_i(\tau)$, propagated from $\Psi_{T,i}$.
- Calculate and normalization matrix elements as functions of τ:

$$H_{ij} = \frac{< \Psi_i(\tau/2) | H | \Psi_j(\tau/2) >}{|\Psi_i(\tau/2)||\Psi_j(\tau/2)|}$$

$$N_{ij} = \frac{< \Psi_i(\tau/2) | \Psi_j(\tau/2) >}{|\Psi_i(\tau/2)||\Psi_j(\tau/2)|}$$

- Solve the generalized eigenvalue problem with these Hamiltonian and normalization matrices.
- Let τ go to ∞.

Energies of Nuclear States

The *absolute* energies of nuclear states calculate in VMC and GFMC for $A = 4 - 12$, with AV18 and IL2 (3N)

- VMF gives reasonable agreement with data
- GFMC gives extremely good agreement with data for many low-lying levels

Comparison of GFMC with No-Core Shell Model Calculations (NCSM)

- NCSM introduces *effective* two-body and three-body interactions in much the same way as V_{lowk}

  Use of the unitary transformation method
- Cutoff is specified by $n\hbar\omega$ rather than the momentum cutoff Λ.
- Once the effective interactions are derived, one can carry out exact diagonalization within the specified model space.
- Without 3N forces, the two methods give comparable results.
- With 3N forces included, GFMF does better than NCSM (with a currently practical choice of $n\hbar\omega$

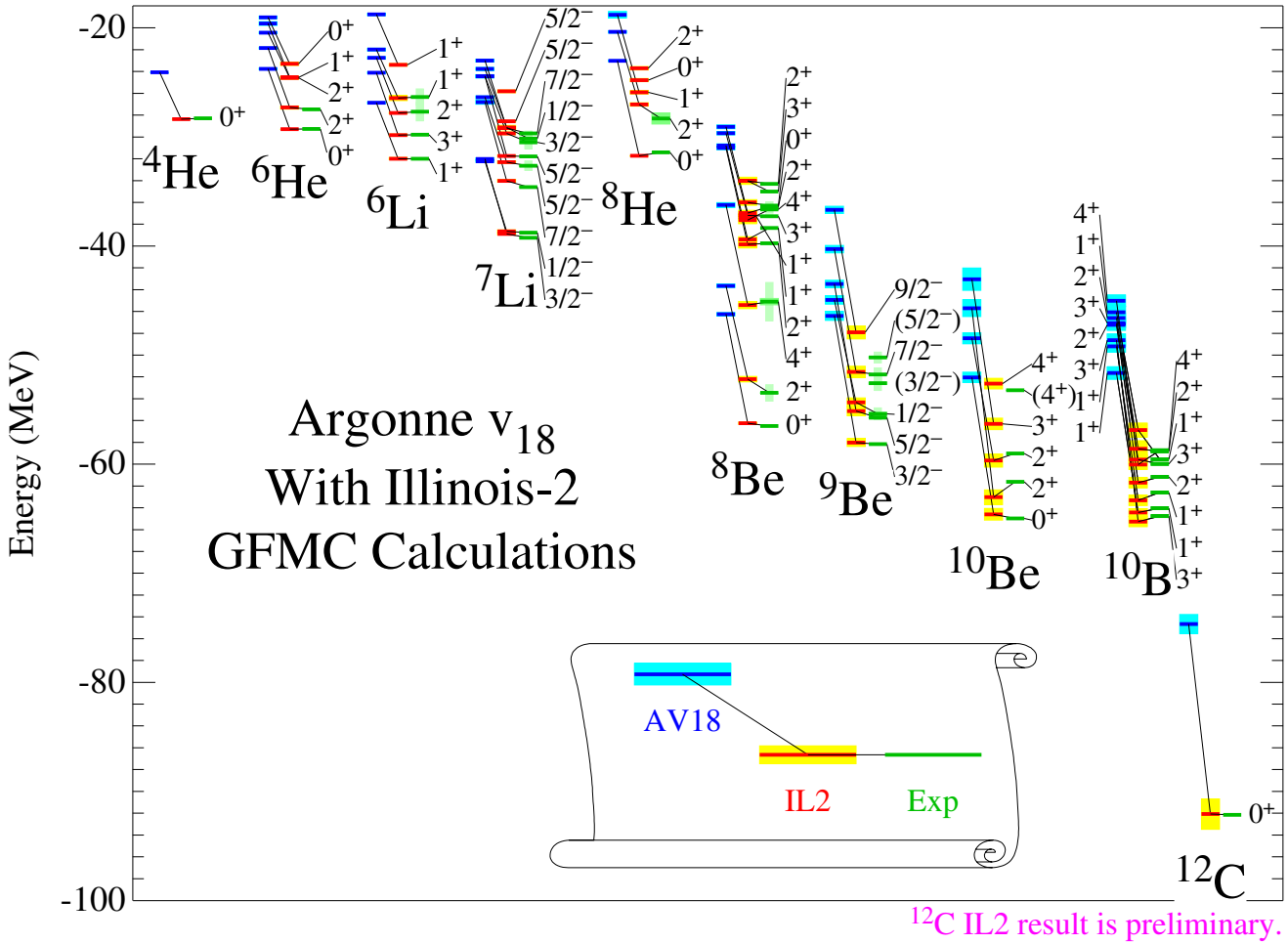

Figure: Energies of nuclear states computed with just the AV18 NN potential, and with the addition of the IL2 NNN potential, compared to experiment.

S. C. Pieper Nucl.Phys. A751 (2005) 516

Table: GFMC calculations of the ^{10}Be ground-state energy E_{gs}, excitation energies E_x (both in MeV), and $B(E2\downarrow)$ transitions in e^2 fm^4.The calculations were done with a variety of potentials to explore the sensitivity in predicting electromagnetic matrix elements.

H	AV18	AV18+UIX	AV18+IL2	AV18+IL7	Expt.
$\lvert E_{gs}(0^+)\rvert$	50.1(2)	59.5(3)	66.4(4)	64.3(2)	64.98
$E_x(2_1^+)$	2.9(2)	3.5(3)	5.0(4)	3.8(2)	3.37
$E_x(2_2^+)$	2.7(2)	3.8(3)	5.8(4)	5.5(2)	5.96
$B(E2; 2_1^+ \rightarrow 0^+)$	10.5(3)	17.9(5)	8.1(3)	8.8(2)	9.2(3)
$B(E2; 2_2^+ \rightarrow 0^+)$	3.3(2)	0.35(5)	3.3(2)	1.7(1)	0.11(2)
$\Sigma B(E2)$	13.8(4)	18.2(6)	11.4(4)	10.5(3)	9.3(3)

The lifetime of the 2_2^+ state in ^{10}Be was also measured. New *ab-initio* calculations show the sensitivity of the transition matrix elements to nuclear structure, especially to the form of $3N$ forces.

McCutchan et al., Phys. Rev. Lett. 103, 192501 (2009)

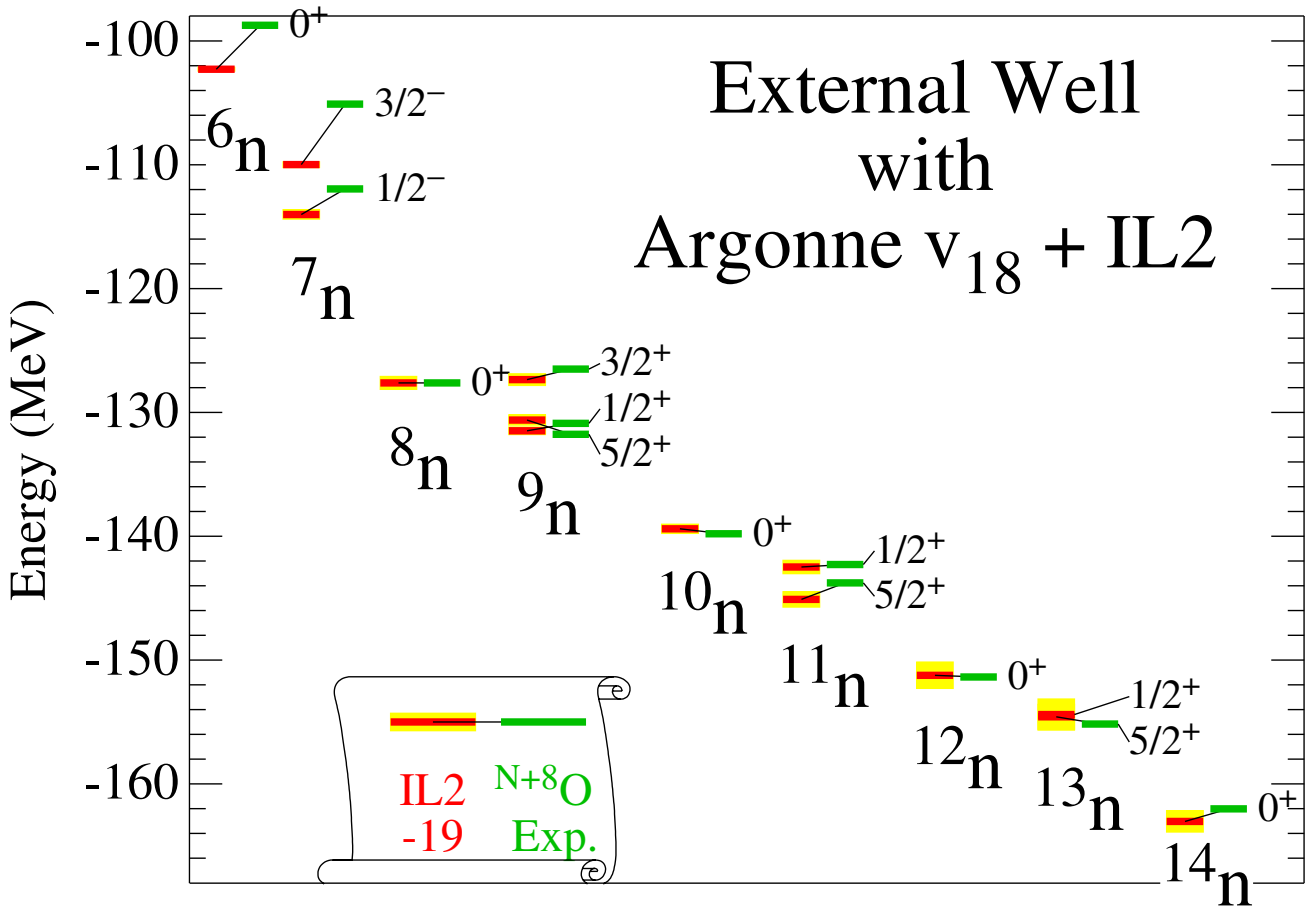

Figure: Energies of neutron drops compared to the corresponding oxygen isotope experimental energies.

S. C. Pieper Nucl.Phys. A751 (2005) 516